3-Aminopyrazole Inhibitors of CDK2/Cyclin A as Antitumor Agents. 1. Lead Finding

Paolo Pevarello,*,† Maria Gabriella Brasca,† Raffaella Amici,† Paolo Orsini,† Gabriella Traquandi,† Luca Corti,† Claudia Piutti,† Pietro Sansonna,† Manuela Villa,† Betsy S. Pierce,‡ Maurizio Pulici,† Patrizia Giordano,† Katia Martina,† Edward L. Fritzen,‡ Richard A. Nugent,‡ Elena Casale,† Alexander Cameron,† Marina Ciomei,§ Fulvia Roletto,# Antonella Isacchi,# GianPaolo Fogliatto,# Enrico Pesenti,§ Wilma Pastori,§ Aurelio Marsiglio,§ Karen L. Leach,|| Paula M. Clare,|| Francesco Fiorentini,⊥ Mario Varasi,† Anna Vulpetti,† and Martha A. Warpehoski‡

Chemistry, Pharmacology, Biology, and Global Drug Metabolism Departments, Pharmacia Italia, Viale Pasteur 10, 20014 Nerviano (MI), Italy, and Chemistry and Pharmacology Departments, Pharmacia Corporation, 301 Henrietta Street, Kalamazoo 49001, Michigan

Received December 17, 2003

Abnormal proliferation mediated by disruption of the normal cell cycle mechanisms is a hallmark of virtually all cancer cells. Compounds targeting complexes between cyclin-dependent kinases (CDK) and cyclins, such as CDK2/cyclin A and CDK2/cyclin E, and inhibiting their kinase activity are regarded as promising antitumor agents to complement the existing therapies. From a high-throughput screening effort, we identified a new class of CDK2/cyclin A/E inhibitors. The hit-to-lead expansion of this class is described. X-ray crystallographic data of early compounds in this series, as well as in vitro testing funneled for rapidly achieving in vivo efficacy, led to a nanomolar inhibitor of CDK2/cyclin A (*N*-(5-cyclopropyl-1*H*-pyrazol-3-yl)-2-(2-naphthyl)acetamide (**41**), PNU-292137, IC_{50} = 37 nM) with in vivo antitumor activity (TGI > 50%) in a mouse xenograft model at a dose devoid of toxic effects.

Introduction

The importance of the retinoblastoma (Rb) pathway in controlling normal cell proliferation has been clearly established.[1,2] The cyclin-dependent kinases (CDKs) are intimately involved in this process.[3] These serine−threonine protein kinases govern the initiation, progression, and completion of cell cycle events. In human cancers, the Rb pathway is universally disrupted either by CDK4 amplification, cyclin D overexpression, mutation of the RB gene, or inactivation of the CDK4 specific inhibitor $p16^{INK4A}$.[4] As a consequence of these alterations, the distribution of the endogenous CDK inhibitor p27 between CDK4 and CDK2 can occur, resulting in an "activation" of CDK2 catalytic activity.[5] The effect of these changes is the deregulation of the transcription factor E2F causing an increased expression of E2F target genes.[6,7] Among these genes are those encoding cyclins A and E as well as other proteins required for DNA replication.

The CDK2 protein can form complexes with both cyclins E and A, and it is required for the G1/S transition and S phase progression[8,9] and centrosome duplication.[10] In addition to being required to maintain Rb phosphorylation, CDK2 also phosphorylates other cell cycle substrates such as Hira, NPAT, and nucleophosmin.[11−13] The microinjection of specific CDK2, cyclin A or cyclin E antibodies, or antisense oligonucleotides will block the cell cycle in normal cells as well as in cells from which Rb has been deleted.[14] This is in contrast to CDK4/cyclin D for which a key role has been demonstrated only in phosphorylating Rb, and therefore, its activity is essential only in Rb positive cells.

One of the key CDK2 substrates is the E2F-1 protein itself, of which the turnover and activity is induced by phosphorylation by CDK2/cyclin A. This leads to higher than normal levels of E2F, which have been found to induce apoptosis.[17] It has been shown that CDK2/cyclin A inactivation through "transfection" of a specific peptide mimetic will induce apoptosis in cells constitutively expressing E2F1.[18] Furthermore, apoptosis is observed in transformed but not in normal cells. Even if these data should be taken with caution, since it is not clear whether a small-molecule catalytic inhibitor of CDK2 will have the same effect as this peptide, they provide a basis for a context-driven therapeutic window upon treatment with a CDK2 inhibitor: tumor cells with a deregulated E2F1 function should be more sensitive than normal cells to a CDK2 inhibitor.

Other observations supporting the use of a CDK2/cyclins E and A inhibitor in a clinical setting rest upon several lines of evidence showing an altered regulation of CDK2, cyclins E and A, and their natural inhibitors ($p21^{CIP2}$ and $p27^{KIP1}$) in human cancers. In particular, overexpression of cyclin A and/or cyclin E has been detected in ∼50% of breast and lung cancers and cyclin E expression becomes progressively higher with increasing stage and grade and correlates with a poor prognosis.[19]

Natural CDK2 kinase inhibitors such as $p27^{KIP1}$ are often unregulated and expressed at low levels in cancer.

* To whom correspondence should be addressed. Phone: +39-0248383481. Fax: +39-0248383937. E-mail: paolo.pevarello@pharmacia.com.
† Chemistry Department, Pharmacia Italia.
‡ Chemistry Department, Pharmacia Corporation.
§ Pharmacology Department, Pharmacia Italia.
# Biology Department, Pharmacia Italia.
|| Pharmacology Department, Pharmacia Corporation.
⊥ Global Drug Metabolism Department, Pharmacia Italia.

10.1021/jm031145u CCC: $27.50
Published on Web 05/15/2004

Chart 1

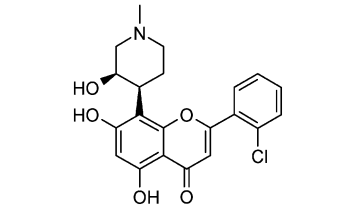

Flavopiridol

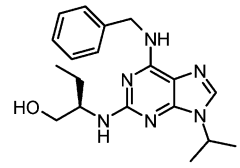

CYC-202

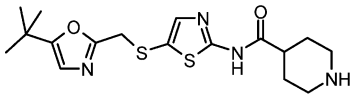

BMS-387032

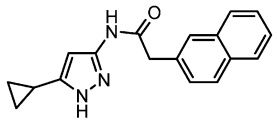

PNU-292137 (41)

Decreased levels of p27 predict a poor prognosis in breast, prostate, colon, gastric, lung, and esophageal cancer.[20]

Thus, although a recent paper suggests that CDK2 activity may not be an absolute requirement for proliferation in some types of tumor cells,[21] there is considerable support to the notion that deregulated activity of CDK2 complexes drives tumor cell growth, and therefore, specific inhibition of CDK2/cyclins A and E kinase activity will block tumor cell proliferation.

Several classes of CDK inhibitors have been described recently in the literature,[22] but so far only a few molecules have progressed into human clinical trials, notably the nonselective CDK inhibitor flavopiridol,[23] the purine analogue (*R*)-roscovitine (CYC-202),[24] and the 2-aminothiazole derivative BMS-387032 (Chart 1).[25]

This paper reports on the discovery of a new class of CDK2 inhibitors and its rapid optimization in potency leading to a compound (**41**, PNU-292137, Chart 1) with good in vivo bioavailability and efficacy in an animal tumor model.

Chemistry

Final compounds were made using two different protocols: (A) coupling of a suitable 5-substituted 3-aminopyrazole with an acid chloride followed by selective basic deacylation of the endocyclic residue to yield the final compounds **1**−**7** and **10**−**29** (Scheme 1); (B) coupling of a suitable 1-Boc protected 5-substituted 3-aminopyrazole[26,27] with a carboxylic acid and a condensing agent followed by the protecting group removal to yield the final compounds **30**−**37** and **40**−**42** (Scheme 2).

According to procedure A, an excess of the acylating agent allowed us to obtain the disubstituted derivative,

Scheme 1[a]

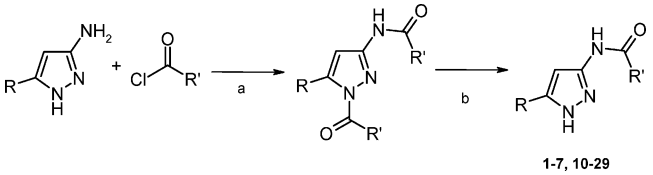

[a] Conditions: (a) CH_2Cl_2, NMM, room temp; (b) MeOH, H_2O, NaOH, room temp.

Scheme 2[a]

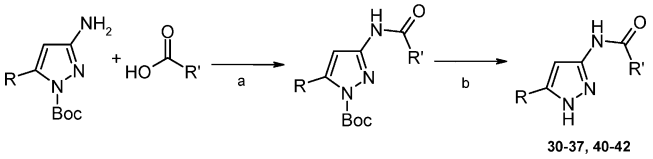

[a] Conditions: (a) EDCl, CH_2Cl_2, room temp; (b) TFA/CH_2Cl_2 (1:9 v/v), room temp.

which is susceptible to selective hydrolysis of the more labile endocyclic position under mild conditions. As outlined in procedure B, 1-Boc protected 5-substituted 3-aminopyrazole was treated with the suitable carboxylic acid by using EDCI as a condensing agent. The resulting intermediate was then deprotected with TFA at room temperature. It is noteworthy that procedure B allowed us to save an equivalent of reactant and to exploit a larger number of stable and commercially available carboxylic acids.

The carbomethoxy derivatives **43** (method A) and **44** (method B) afforded, respectively, compounds **8** and **38** by basic hydrolysis (Scheme 3) and compounds **9** and **39** by ammonolysis (Scheme 4).

5-Substituted 3-aminopyrazole precursors of final compounds **1**−**42** and carboxylic acid derivatives employed to obtain final compounds **1**−**32** and **34**−**42** were either commercially available or known from the literature and are reported in the Registry Numbers section. [4-(2-Pyrrolidin-1-yl-ethoxy)phenyl]acetic acid (**47**) was prepared from 4-hydroxyphenylacetic acid by a three-step sequence as described in Scheme 5.

Biological and Preliminary ADME Testing Scheme

Compounds were tested according to a screening funnel, the entry point being a biochemical assay for inhibition of CDK2/cyclin A. Compounds having IC_{50} values lower than approximately 100 nM were subsequently tested for their antiproliferative activity against A2780 human ovarian tumor cells. Compounds with an IC_{50} in the low micromolar range were further characterized in vitro for their ability to block the cell cycle by fluorescence activated cell sorting (FACS) and DNA synthesis by bromodeoxyuridine (BrdU) incorporation block of A2780 cells, as well for their ability to block other tumor cell lines (HT-29, DU145, and HCT-116). In parallel, an assessment of drug parameters such as buffer solubility, CYP4503A4 inhibition, cell permeability, and plasma protein binding was conducted. Selected compounds were tested for their selectivity against a panel of kinases. By integrating in vitro biological and pharmacological results and preliminary absorption, disposition, metabolism, and excretion (ADME) parameters and after having assessed in vivo

Scheme 3[a]

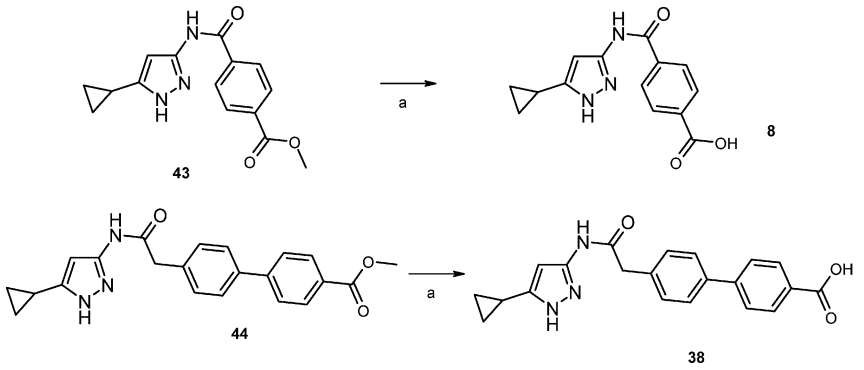

[a] Conditions: (a) aqueous KOH, THF.

Scheme 4[a]

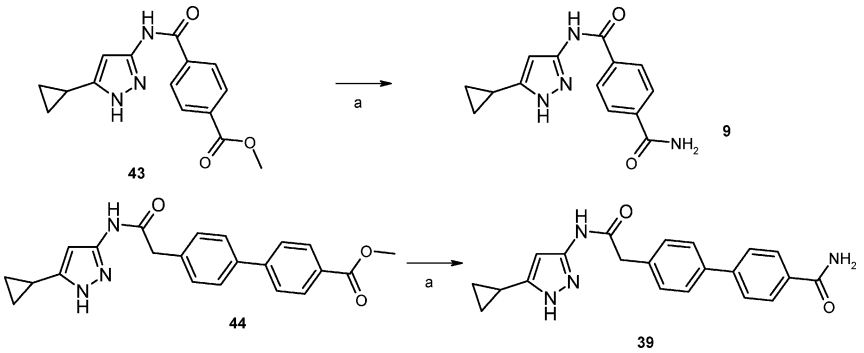

[a] Conditions: (a) NH_3, MeOH, $DMF_{cat.}$, 60 °C.

Scheme 5[a]

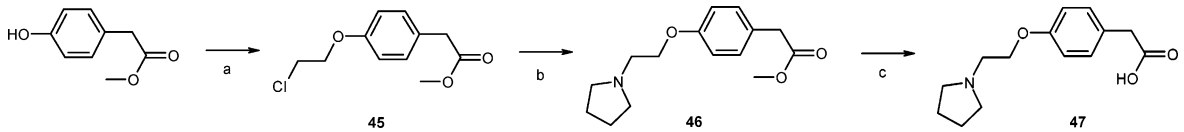

[a] Conditions: (a) $Cl-(CH_2)_2-Br$, K_2CO_3, acetone, reflux; (b) pyrrolidine, KI, DMF, 100 °C; (c) 1 N NaOH, room temp.

pharmacokinetic (PK) parameters in rats, a lead compound (**41**) was selected for in vivo assessment in an animal tumor model (A2780 xenograft tumor).

Results and Discussion

Among several classes of potential CDK2/cyclin A inhibitors emerging from an internal high-throughput screening (HTS) effort, we focused our attention on 3-aminopyrazoles because of the low molecular weight of the scaffold and amenability for rapid class expansion. Initial hits **1**−**4** (Table 1) allowed a preliminary, albeit rough structure−activity relationship (SAR) evaluation: (1) a cyclopropyl substituent at position 5 of the 3-aminopyrazole scaffold was much more effective than a methyl group (**2** vs **3**) when an *n*-propylamide was the residue at position 3, and it still conferred a significantly enhanced potency with a 3-benzamido group (**1** vs **4**). (2) a 3-benzamido compound (**4**) also had a good activity as a CDK2/cyclin A inhibitor, considerably widening the number of products that could be evaluated during class expansion. The crystal structure of CDK2 with compound **4** was determined (Figure 1). From this, it was observed that the three nitrogens of the 3-aminopyrazole scaffold were involved in a donor−acceptor−donor hydrogen bond triad, making contact with the hinge region (Glu81-Leu83) of the kinase ATP pocket. The 5-cyclopropyl ring occupies the narrow lipophilic pocket formed by Val18, Ala31, Val64, and Phe80. The plane of the cyclopropyl ring is almost perpendicular to the plane of the pyrazole ring and is packed nicely against the phenyl ring of Phe80. Finally the benzene ring of **4** is directed toward the solvent-accessible region of the enzyme pocket, contributing to the overall binding through lipophilic interactions with the side chains of Ile10 and Phe82 and the main chain of His84 and Asp86.

From a medicinal chemistry perspective, where a rapid expansion of the chemical class is important, it was thought that the choice of the 5-substituent was likely to be restricted to groups able to be accommodated into the narrow lipophilic pocket, while there was considerable room for a quick expansion associated with the 3-substituent. This turned out to be true as we proceeded with class expansion. Furthermore, modeling work suggested that generic substitution at position 4 may be detrimental for activity, since it would force the 3-aminocarbonyl group into a conformation that would disrupt the hydrogen-bonding of the 3-aminopyrazole to the hinge region of the enzyme.

The SAR associated with different substituents on the 3-benzamido moiety was first investigated. Compounds **5**−**9** showed that substituents at the para position of

Table 1. SAR of of 3-Propylamido- and 3-Benzamidoaminopyrazoles (**1**−**29**)

compd	R	R_1	CDK2/cyclin A (IC_{50}, nM)[a]
1	methyl	phenyl	1500
2	methyl	propyl	>10000
3	cyclopropyl	propyl	224
4	cyclopropyl	phenyl	290
5	cyclopropyl	4-Br−C_6H_4−	34
6	cyclopropyl	4-Cl−C_6H_4−	85
7	cyclopropyl	4-OMe−C_6H_4−	705
8	cyclopropyl	4-COOH−C_6H_4−	165
9	cyclopropyl	4-$CONH_2$−C_6H_4−	68
10	cyclopropyl	3-Br−C_6H_4−	990
11	cyclopropyl	3-Cl−C_6H_4−	1000
12	cyclopropyl	3-OMe−C_6H_4−	600
13	cyclopropyl	3-CF_3−C_6H_4−	500
14	cyclopropyl	2-Br−C_6H_4−	1500
15	cyclopropyl	2-Cl−C_6H_4−	1000
16	cyclopropyl	2-OMe−C_6H_4−	>10000
17	cyclopropyl	2,6-diCl−C_6H_4−	>10000
18	cyclopropyl	3,4-diCl−C_6H_4−	83
19	cyclobutyl	4-Br−C_6H_4−	90
20	cyclopentyl	4-Br−C_6H_4−	50
21	cyclohexyl	4-Br−C_6H_4−	1000
22	methyl	4-Br−C_6H_4−	6000
23	ethyl-	4-Br−C_6H_4−	630
24	propyl	4-Br−C_6H_4−	650
25	isopropyl	4-Br−C_6H_4−	200
26	*sec*-butyl	4-Br−C_6H_4−	>10000
27	*tert*-butyl	4-Br−C_6H_4−	>10000
28	phenyl	4-Br−C_6H_4−	>10000
29	benzyl	4-Br−C_6H_4−	>10000

[a] See Experimental Section.

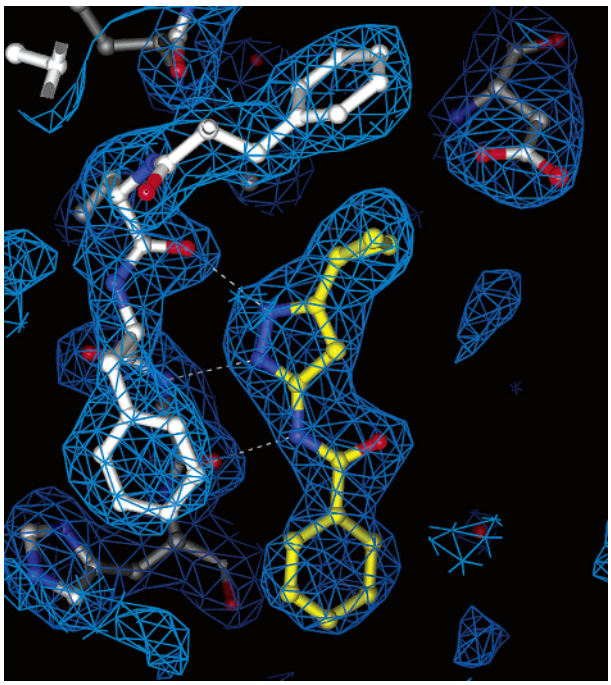

Figure 1. ATP binding pocket residues of the X-ray structure of CDK2 in complex with **4**. The three hydrogen bonds between the CDK2 hinge region and the inhibitor are drawn as dashed lines.

the benzamido ring retained or favored potency compared to the unsubstituted compound **4**, giving IC_{50} values in the range 34−705 nM. Halogen substituents and electron-withdrawing groups provided the best results.

We then examined the effect of substitution at positions 2 and 3 on the benzamido moiety (**10**−**18**). We observed a clear drop in activity compared to the unsubstituted parent compound **4**. The potency of the 3,4-dichlorobenzamide derivative (**18**) shows that the presence of a 4-chloro is able to offset the loss in activity that is brought about by the 3-chloro substituent. A steric clash between a 2-substituent on the benzamido ring and the amino acid residues lining the hinge region of the enzyme is likely to account for this clear-cut SAR (e.g., **16** and **17**), while the reason for the diminished activity of the 3-substituted benzamides (**10**−**13**) is not clear even after model inspection.

We then turned our attention to the effect of different 5-substituents on a series of 3-(4-bromobenzamido)-pyrazoles (**5**, **19**−**29**), and we confirmed that small cycloalkyl groups (**5**, **19**, **20**) gave the best inhibitions. C_2 and C_3 alkyl groups retained some activity, while smaller (**22**) and larger linear or branched alkyl or cycloalkyl groups (**21** and **26**−**29**) were detrimental to a good inhibitory effect.

This finding is consistent with the observed binding mode of this class, since alkyl and aryl substituents other than small cycloalkyl groups would interact unfavorably with Phe80.

On further expansion of this chemical class, we looked at the effect of a phenylacetamido moiety on the 3-aminopyrazole scaffold. A selection of 3-phenylacetamido derivatives is reported in Table 2, and low nanomolar activity is frequently met in this subclass. Structural inspection of this region suggested that a phenylacetic residue would give a more favorable interaction with the lipophilic Ile10 and Phe82 amino acid residues on the rim of the solvent-accessible region. In fact, the 2-benzylcarbonylamino moiety in position 3 of the pyrazole perfectly mimics the interaction of the *N*-6-benzyl group present in the purine CDK2 inhibitors, such as roscovitine or olomucine, with the protein.[28] To confirm this hypothesis, the crystal structure of **41** in complex with CDK2/cyclin A was determined (Figure 2). In Figure 3a, **41** and (*R*)-roscovitine are shown superimposed in the ATP binding pocket of CDK2/cyclin A. The superposition shows that the substituents of two different scaffolds, the 3-aminopyrazole and the purine, can be placed in identical positions with respect to the protein. As shown in Figure 3a, the cyclopropyl of **41** and the isopropyl of (*R*)-roscovitine overlap perfectly and make similar interactions with the hydrophobic pocket at the back of the CDK2 ATP pocket. Furthermore the naphthyl moiety of **41** lies in the same plane as the phenyl moiety of the (*R*)-roscovitine *N*-6-benzyl group, allowing hydrophobic interactions with the side chains of Ile 10 and Phe82 (Figure 3b). It should also be noted that the conformational changes in the PSTAIRE helix and in the T-loop of CDK2, due to cyclin A binding,[29] occur far from the bound 3-amidopyrazole ligands. Consequently, the presence or absence of cyclin A does not appear to affect the binding mode of the inhibitors, as demonstrated by a comparison of the binding modes of the two pyrazole derivatives **4** and **41** in complex with CDK2 and CDK2/cyclin A, respectively (Figure 2).

Despite the good activity attained in the biochemical assay for CDK2/cyclin A inhibition, all compounds reported in Table 1 displayed weak activity in a tumor cell antiproliferation test (A2780 human ovarian tumor cells), with IC_{50} values in the medium−high micromolar

Table 2. SAR of of 3-Phenylacetamidoaminopyrazoles (**30**−**42**)

compd	R	R_1	CDK2/cyclin A (IC_{50}, nM)[a]	A2780 cells (IC_{50} ± SD, nM)
30	cyclopropyl	phenylacetyl	48	1400 ± 112
31	cyclopropyl	4-$conh_2$-phenylacetyl	74	2835 ± 235
32	cyclopropyl	3-ome-phenylacetyl	29	>20000
33	cyclopropyl	4-(2-pyrrolidin-1-yl)-ethoxy	95	6984 ±813
34	cyclopropyl	4-OCF_3-phenylacetyl	67	4990 ± 570
35	cyclopropyl	4-biphenylacetyl	56	111 ± 39
36	cyclopropyl	4-(3-fluorobiphenyl)acetyl	4	182 ± 3
37	cyclopropyl	4-(3-methylbiphenyl)acetyl	9	205 ± 7
38	cyclopropyl	4-(4-carboxybiphenyl)acetyl	11	>20000
39	cyclopropyl	4-(4-carboxamidobiphenyl)acetyl	4	1468 ± 165
40	cyclopropyl	4-(2-thenyl)-phenylacetyl	3	121 ± 3
41	cyclopropyl	4-(2-naphthyl)acetyl	37	286 ± 49
42	cyclopropyl	4-(1-naphthyl)acetyl	38	900 ± 112

[a] See Experimental Section.

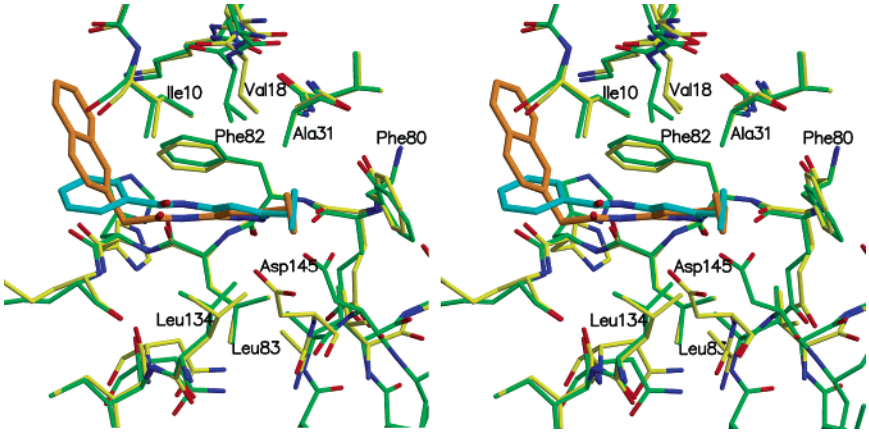

Figure 2. Stereoview showing the structure of CDK2 complexed with compound **4** (green carbon atoms for the protein, cyan carbon atoms for the inhibitor) superimposed on the structure of CDK2/cyclin A with compound **41** (yellow carbon atoms for the protein, orange for the inhibitor). It is clear from this figure that compound **41** retains the same hydrogen-bonding pattern as observed for **4**. The benzylic methylene of the naphthylacetamide group of **41** with respect to the benzoic group of **4** allows this substituent to adopt a bent conformation with the naphthyl group packing onto Ile10. The differences in the conformations of the protein residues are caused by having cyclin bound in one case and not in the other. This does not appear to affect the binding of the ligand.

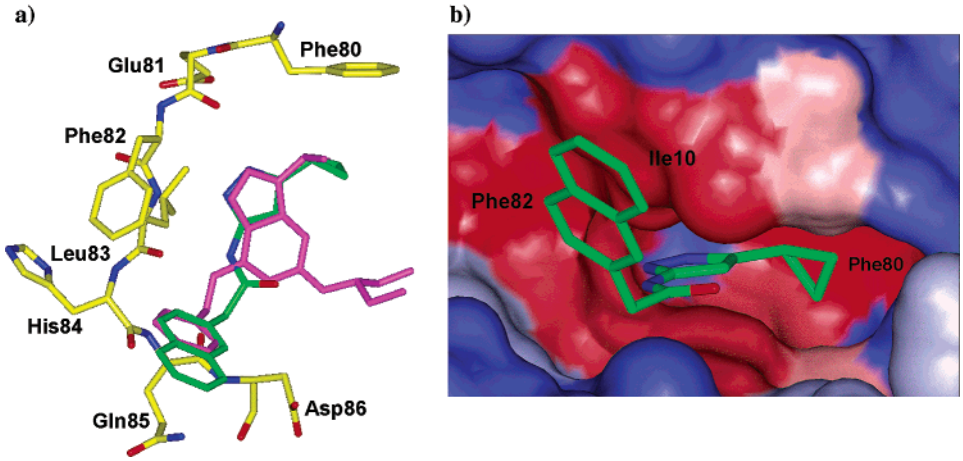

Figure 3. Crystal structure of **41** in complex with CDK2/cyclin A: (a) overlap of **41** (atom-type colored) and roscovitine (magenta) complexed to CDK2/cyclin A; (b) surface representation of ATP binfing cleft, colored by residue hydrophobicity, in complex with **41**. Red indicates most hydrophobic residues, and blue indicates the most polar ones.

range. On the other hand, several compounds in Table 2 are endowed with potent cellular activity. The SAR, linking activity in the biochemical assay with cellular activity on the basis of the physicochemical properties of a molecule, is often difficult to rationalize because many variables are known to play a role. In addition to cellular membrane permeability and subcellular compartmentalization, tumor cells possess refined mechanisms for efficiently extruding xenobiotica.[30] It is not uncommon, therefore, to observe that even minor modifications in otherwise very similar compounds lead to dramatic differences in cellular activity.[31] Compound **35** exemplifies this fact very well in that by simply replacing the phenylacetoamide moiety of **30** with a biphen-

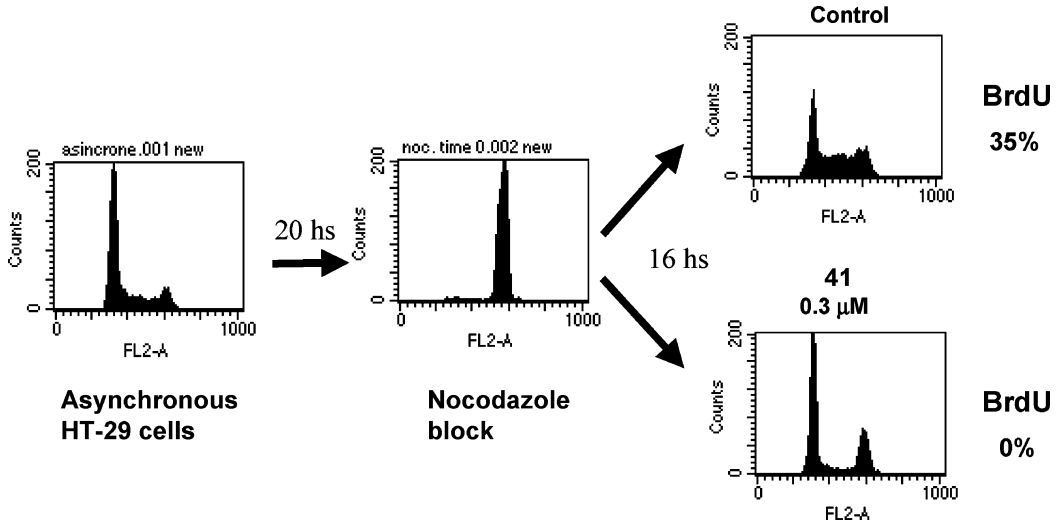

Figure 4. **41** blocks cell cycle progression. Cells synchronized in G2/M by nocodazole treatment were released in the absence or in the presence of **41**. In comparison with the control cells, cells treated with **41** showed a block in G1 and a complete absence of S phase, as confirmed by the lack of BrdU incorporation.

Table 3. Antiproliferative Activity of **41** on Different Human Tumor Cell Lines ($IC_{50} \pm$ SD, nM)

compd	A2780 cells	HT-29 cells	HCT116 cells	DU145 cells
41	286 ± 49	170 ± 1	73 ± 30	651 ± 89

ylacetamido residue (**35**), we achieved potent nanomolar antiproliferative activity on A2780 cells (Table 2). While increased lipophilicity and improved cell membrane permeability can partially account for a better cellular activity of **35** vs **30**, the experimental result has yet to be fully rationalized. Compound **35**, while pharmacologically very potent, had poor physicochemical properties (e.g., buffer solubility in the single-digit micromolar range and plasma protein binding close to 100%), hampering its use as an in vivo tool for investigating antitumor activity of a CDK2/cyclin A inhibitor in a xenograft model.

Several biarylacetamido derivatives (**36**−**40**, Table 2) were shown to be single-digit nanomolar inhibitors in the biochemical assay for CDK2/cyclin A inhibition, and some of them also displayed potent antiproliferative activity, but an overall druglike profile compatible with a possible in vivo evaluation was achieved only with the 2-naphthyl derivative **41** (Table 5).

This compound proved to be a valuable tool for understanding the potential of CDK2/cyclin A inhibitors in an in vivo antitumor setting and was further submitted for (a) inhibition of tumor cell proliferation in different tumor cell lines, (b) cell cycle analysis, (c) preliminary ADME and in vivo PK parameters, (d) kinase selectivity profile, and (e) in vivo evaluation in the A2780 human ovarian tumor xenograft model.

(a) Inhibition of Tumor Cell Proliferation in Different Tumor Cell Lines. Activity of **41** in a broader panel of tumor cell lines was assessed (Table 3), and the compound was found to efficiently inhibit tumor cell proliferation in human colon (HT-29 and HCT-116) and prostate (DU145) tumor cell lines with a potency comparable with that observed in A2780 cells.

(b) Cell Cycle Analysis. Further in vitro investigation was aimed at demonstrating that the antiproliferative activity observed was mediated by CDK2 inhibition. The cell cycle profile was studied using FACS, after synchronization with nocodazole. Cell population peaks showed a G1 block at 0.3 μM (Figure 4) with total block of BrdU incorporation, meaning that DNA synthesis in these tumor cells was impaired. Western blot analysis of the phosphorylation status of the known substrate, retinoblastoma protein (pRb), showed a corresponding block of the phosphorylation at 0.1−0.3 μM (Figure 5), adding further evidence to the notion that antiproliferation activity of **41** is mediated by blocking CDK2.

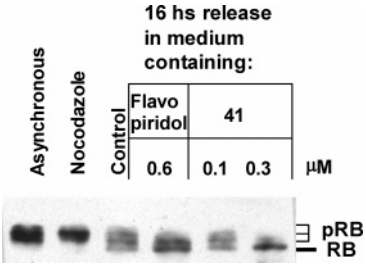

Figure 5. **41** blocks pRB phosphorylation. After the treatment with 0.3 μM **41**, the substrate retinoblastoma protein (pRb) is mainly in the dephosphorylated form.

(c) Kinase Selectivity Profile. Compound **41** was assessed for its selectivity against a panel of 33 kinases (Table 4). Among the members of the CDK family that were tested, it was found to inhibit CDK2/cyclin E, CDK5/p25, and less potently CDK1/cyclin B, but it displayed selectivity for CDK4/cyclin D1. Compound **41** had a 60-fold higher IC_{50} versus GSK-3β, while IC_{50} values for all other enzymes in the panel were higher than 10 μM. The overall good selectivity profile reinforced the value of **41** as a candidate for further in vivo evaluation in an efficacy model.

(d) Preliminary ADME and in Vivo Pharmacokinetic (PK) Parameters. Compounds of this series were routinely assessed on tests predictive of good druglike properties. The parameters of **41** (Table 5) were consistent with a good predicted in vivo bioavailability. The compound was then assessed in a preliminary PK study in rats mice, and in vivo clearance, volume of

Table 4. Selectivity Profile of **41** on a Panel of 33 Kinases

kinase	IC_{50} (nM)	enzyme concn (nM)	substrate	buffer	assay format
CDK2/cyclin A	37	1.1	HISTONE H1	A	SPA
CDK2/cyclin E	92	1.1	HISTONE H1	A	SPA
CDK5/p25	114	4	HISTONE H1	A	SPA
CDK1/cyclin B	270	4	HISTONE H1	A	SPA
CDK4/cyclin D1	>10000	60	RB	A	multiscreen
ABL	>10000	1.2	MBP	B	SPA
AKT-1	>10000	5	AKTtide	A	Dowex
AUR-2	>10000	2.5	CHOCKtide 4X	C	SPA
CDC7/DBF4	>10000	18	MCM2	C	SPA
CHK-1	>10000	12	CHKtide	B	SPA
CK-2	>10000	0.7	MCM2	C	SPA
EGFR-1	>10000	9	MBP	B	SPA
ERK-2	4600	3	MBP	A	Dowex
FGFR-1	>10000	4	MBP	B	SPA
GSK-3β	1905	20	MBP	B	SPA
IGFR-1	>10000	6	IRStide	D	SPA
IKK-2	>10000	15	IKBalpha	C	SPA
IKKi	>10000	5	IKBalpha	B	Dowex
IR	>10000	5	IRStide	C	SPA
KIT	>10000	4	KITtide	B	SPA
LCK	>10000	1.3	MBP	B	SPA
LYN	>10000	2	HISTONEH1	B	SPA
MET	>10000	10	MBP	B	Dowex
p38α	>10000	5	MBP	B	Dowex
PAK4	>10000	2	PAKtide	B	SPA
PDGFR-1	>10000	9	MBP	B	SPA
PDK1	>10000	15	PDKtide	C	SPA
PKCβ	>10000	2	HISTONE H1	B	SPA
PLK1	>10000	50	αCASEIN	E	Dowex
RET	>10000	5	MBP	B	SPA
STLK2	>10000	1	MBP	B	SPA
TRKA	>10000	1.5	MBP	B	Dowex
VEGFR-2	>10000	4.7	MBP	D	SPA
VEGFR-3	>10000	10	MBP	B	SPA
ZAP70	>10000	8	GASTRIN	D	SPA

Table 5. Solubility, Cellular Permeability, Predicted Clearance, and Plasma Protein Binding (PPB) of **41**

buffer solubility (μM) (pH 7)	cellular permeability (Caco-2)	metabolic rate (mL min^{-1} kg^{-1}) (rat hepatocytes)	plasma protein binding (%) (HSA)
22	high	27.8	99

Table 6. Pharmacokinetic Parameters of **41** after Intravenous and Oral Administration to Male Sprague Dawley Rats

	iv administration	oral (po) administration
dose (mg/kg)	5	10
dose (nmol/kg)	17161	34322
C_{max} (nM)	19.4 ± 3.9	9.63 ± 1.81
T_{max} (h)		1.39 ± 0.53
AUC_{tot} (μM·h)	21.24 ± 1.45	38.18 ± 8.15
$T_{1/2}$ (h)	1.0 ± 0.17	2.38 ± 1.73
MRT (h)	1.31 ± 0.34	
clearance (mL min^{-1} kg^{-1})	13.5 ± 0.98	
V_{ss} (mL kg^{-1})	1057 ± 278	
bioavailability (%)		89.8

distribution, half-life, and high oral bioavailability warranted its use in an in vivo efficacy model (Table 6).

(e) In Vivo Evaluation in the A2780 Human Ovarian Xenograft Tumor. 41 was evaluated in an in vivo model of antitumor activity on nu/nu mice bearing human ovarian A2780 xenografted tumors. The compound was administered orally (10 mg/kg daily and 7.5 mg/kg, b.i.d., for 10 days) (Figure 6), yielding a tumor growth inhibition (TGI) of 53% (with the b.i.d. administration schedule) without any significant weight loss and toxicity being observed in the study.

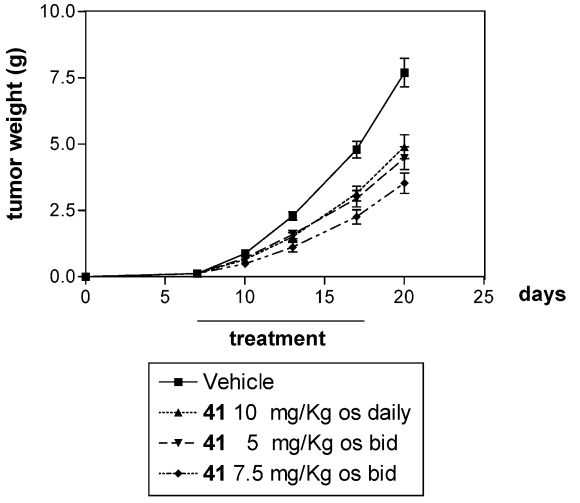

Figure 6. Antitumor efficacy of **41**. Compound **41** shows a 53% tumor growth inhibition (TGI) against a human ovarian cancer model (A2780) transplanted into nude mice when administered at 7.5 mg/kg twice a day for 10 consecutive days.

Conclusion

A novel class of CDK2/cyclin A inhibitors was discovered from HTS and rapidly optimized to an in vivo pharmacological tool that demonstrated tumor growth inhibition in a xenograft model of human ovarian cancer. Structure-based drug design was applied throughout class expansion and was instrumental to direct the synthesis toward more potent inhibitors. Lead compound **41** (PNU-292137) was a valuable tool for demonstrating the potential of CDK2/cyclins E and A inhibitors in an in vivo setting. Its optimization to yield

compounds with an improved druglike profile will be the subject of a future communication.

Experimental Section

I. Chemistry. Melting points were determined in open glass capillaries with a Buchi 535 melting point apparatus and are uncorrected. Elemental analyses were performed on a Carlo Erba 1110 instrument, and C, H, and N results were within ±0.4% of theoretical values. ^{1}H NMR spectra were recorded on a Varian Mercury 400 spectrometer, using the solvent as internal standard; chemical shifts are expressed in ppm (δ). Electron impact (EI) mass spectra (MS) were obtained on a Finnigan-MAT TSQ 700 triple-quadrupole instrument. ESI mass spectra were obtained on LCQ ion trap (thermo), Finnigan. Organic solutions, where applicable, were dried over anhydrous Na_2SO_4 and evaporated using an Heidolph WB 2001 rotary evaporator at 15−20 mmHg. Flash column chromatographic separations were carried out on 40/60 μm silica gel (Carlo Erba). Thin-layer chromatography was performed on Whatman silica gel 60 plates coated with a 250 μm layer with fluorescent indicator. Components were visualized by UV light (λ = 254 nm) by iodine vapor. Dichloromethane was distilled from P_2O_5 and stored over 4 Å molecular sieves. All experiments dealing with moisture-sensitive compounds were conducted under dry nitrogen. Starting materials, unless otherwise specified, were commercially available (Aldrich, Fluka) and of the best grade and were used without further purification.

Method A. *N*-(5-Cyclopropyl-1*H*-pyrazol-3-yl)benzamide (4). To a solution of 0.37 g (3 mmol) of 3-cyclopropyl-5-amino-1*H*-pyrazole in 15 mL of dichloromethane 0.8 mL (7.3 mmol) of *N*-methylmorpholine and 0.8 mL (6.9 mmol) of benzoyl chloride were successively added at room temperature. After 16 h under stirring, the mixture was concentrated and the residue was dissolved in 15 mL of methanol. An amount of 3.5 mL of sodium hydrate, 2.5 M, was added dropwise, and 10 mL of tetrahydrofuran was finally added in order to obtain a homogeneous solution. After 15 min the mixture was concentrated and poured into water. The precipitate was filtered and dried in a vacuum to afford 585 mg (86%) of the title compound: mp 232−234 °C; ^{1}H NMR (DMSO-d_6) δ 12.1 (s, 1H), 10.65 (s, 1H), 7.97 (app d 2H), 7.50 (m, 3H), 6.31 (s, 1H), 1.89 (m, 1H), 0.93 (m, 2H), 0.69 (m, 2H); ^{13}C NMR (DMSO-d_6): 7.2 (CH6, 8.1 (CH2−7, CH2−8), 43.0 (CH2−12), 92.8 (CH-4), 126.9 (CH-16), 128.7 (CH15, CH-17), 129.5 (CH-14, CH-18), 136.7 (C-13), 147.8 (C-5), 168.5 (C-10); MS (EI) *m/z* (rel intensity) 227 (M^+, 22), 226 (11), 199 (23), 106 (13), 105 (95), 78 (11), 77 (99), 66 (9), 65 (14), 51 (29); HRMS (FAB) calcd for $C_{13}H_{13}N_3O$ + H1 228.1131, found 228.1122. Anal. ($C_{13}H_{13}N_3O$) C, H, N.

Analogously, using the corresponding 5-substituted 3-amino-1*H*-pyrazole and a suitable acid chloride, the following compounds were prepared.

***N*-(5-Methyl-1*H*-pyrazol-3-yl)benzamide (1):** yield 58%; mp 218−220 °C; ^{1}H NMR (DMSO-d_6) δ 12.10 (s, 1H), 10.70 (s, 1H), 7.98 (d, 2H), 7.50 (m, 3H), 6.40 (s, 1H), 2.23 (s, 3H); MS (EI) *m/z* (rel intensity) 201 (M^+, 92), 200 (44), 173 (94), 172 (18), 106 (74), 105 (99), 78 (41), 77 (99), 51 (92), 50 (23). Anal. ($C_{11}H_{11}N_3O$) C, H, N.

***N*-(3-Methyl-1*H*-pyrazol-5-yl)butanamide (2):** yield 62%; mp 190−192 °C; ^{1}H NMR (DMSO-d_6) δ 11.89 (bs, 1H), 10.12 (bs, 1H), 6.25 (s, 1H), 2.23 (t, 2H, J = 7.32 Hz), 2.19 (s, 3H), 1.56 (m, 2H), 0.89 (t, 3H, J = 7.32 Hz); MS (EI) *m/z* (rel intensity) 167 (M^+, 20), 149 (15), 97 (100), 96 (23), 43 (13); HRMS (FAB) calcd for $C_8H_{13}N_3O$ + H1 168.1131, found 168.1129. Anal. ($C_8H_{13}N_3O$) C (calcd 57.47, found 56.72), H, N.

***N*-(3-Cyclopropyl-1*H*-pyrazol-5-yl)butanamide (3):** yield 66%; ^{1}H NMR (DMSO-d_6) δ 11.96 (bs, 1H), 10.13 (bs, 1H), 6.14 (s, 1H), 2.05 (m, 2H), 1.85 (m, 1H), 1.57 (m, 2H), 0.7−0.9 (2 m, 7H); MS (ESI+) *m/z* (rel intensity) 216 (MNa^+, 25), 194 (MH^+, 82), 176 (93), 124 (100); HRMS (FAB) calcd for $C_{10}H_{15}N_3O$ + H1 194.1288, found 194.1296. Anal. ($C_{10}H_{15}N_3O$) C (calcd 62.15, found 61.12), H, N.

***N*-(5-Cyclopropyl-1*H*-pyrazol-3-yl)-4-bromobenzamide (5):** yield 25%); mp 186−188 °C; ^{1}H NMR (DMSO-d_6) δ 7.91 (d, J = 8.5 Hz, 2H), 7.68 (d, 2H), 6.29 (s, 1H), 1.88 (m, 1H), 0.90 (m, 2H), 0.67 (m, 2H); MS (EI) *m/z* (rel intensity) 305 (M^+, 27), 185 (99), 183 (39), 183 (68), 157 (44), 155 (49), 77 (38), 76 (41), 66 (42), 51 (29); HRMS (FAB) calcd for $C_{13}H_{12}BrN_3O$ + H1 306.0242, found 306.0238. Anal. ($C_{13}H_{12}BrN_3O$) C, H, N, Br.

***N*-(5-Cyclopropyl-1*H*-pyrazol-3-yl)-4-chlorobenzamide (6):** yield 57%); mp 186−187 °C; ^{1}H NMR (DMSO-d_6) δ 12.2 (s, 1 H), 10.8 (s, 1 H), 7.97 (app d, 2 H), 7.53 (app d, 2 H), 6.28 (s, 1 H), 1.87 (m, 1 H), 0.91 (m, 2 H), 0.67 (m, 2 H); MS (EI) *m/z* (rel intensity) 261 (M^+, 27), 235 (8), 233 (36), 141 (66), 139 (99), 113 (31), 111 (78), 75 (19), 75 (9), 65 (10). Anal. ($C_{13}H_{12}ClN_3O$) C, H, N, Cl.

***N*-(5-Cyclopropyl-1*H*-pyrazol-3-yl)-4-methoxybenzamide (7):** yield 70%; mp 173−175 °C; ^{1}H NMR (DMSO-d_6) δ 12.11 (s, 1H), 10.51 (s, 1H), 7.97 (d, J = 8.8 Hz, 2H), 7.00 (d, J = 8.8 Hz, 2H), 6.26 (s, 1H), 3.80 (s, 3H), 1.86 (m, 1H), 0.91 (m, 2H), 0.67 (m, 2H); MS (EI) *m/z* (rel intensity) 257 (M^+, 32), 257 (32), 229 (14), 135 (99), 107 (19), 92 (38), 77 (58), 74 (15), 73 (18), 65 (17), 64 (18). Anal. ($C_{14}H_{15}N_3O_2$) C, H, N.

***N*-(5-Cyclopropyl-1*H*-pyrazol-3-yl)-3-bromobenzamide (10):** yield 43%; mp 157−158 °C; ^{1}H NMR (DMSO-d_6) δ 12.20 (s, 1H), 10.75 (s, 1H), 8.14 (s, 1H), 7.96 (d, J = 7.9 Hz, 1H), 7.72 (d, 1H), 7.43 (t, J = 7.9 Hz, 1H), 6.28 (s, 1H), 1.87 (m, 1H), 0.918 (m, 2H), 0.675 (m, 2H); MS (EI) *m/z* (rel intensity) 305 (M^+, 16), 185 (99), 183 (99), 157 (45), 155 (50), 77 (39), 76 (53), 75 (22), 66 (31), 65 (17), 51 (24). Anal. ($C_{13}H_{12}BrN_3O$) C, H, N, Br.

***N*-(5-Cyclopropyl-1*H*-pyrazol-3-yl)-3-chlorobenzamide (11):** yield 75%; mp 145−147 °C; ^{1}H NMR (DMSO-d_6) δ 12.35 (s, 1H), 10.80 (s, 1H), 7.50−8.00 (4m, 4H), 6.32 (s, 1H), 1.91 (m, 1H), 0.95 (m, 2H), 0.71 (m, 2H); MS (ESI+) *m/z* (rel intensity) 545 ($2MNa^+$, 5), 262 (MH^+, 100), 244 (22). Anal. ($C_{13}H_{12}ClN_3O$) C, H, N.

***N*-(5-Cyclopropyl-1*H*-pyrazol-3-yl)-3-methoxybenzamide (12):** yield 38%; mp 147−149 °C; ^{1}H NMR (DMSO-d_6) δ 12.15 (s, 1H), 10.65 (s, 1H), 7.55 (d, 2H), 7.39−7.36 (t, J = 8.0 Hz, 1H), 7.10 (app d, 1H), 6.29 (s, 1H), 3.80 (s, 3H), 1.87 (m, 1H), 0.917 (m, 2H), 0.67 (m, 2H); HRMS (FAB) calcd for $C_{14}H_{15}N_3O_2$ + H1 258.1242, found 258.1230.

***N*-(5-Cyclopropyl-1*H*-pyrazol-3-yl)-3-trifluoromethylbenzamide (13):** yield 22%; mp 192−193 °C; ^{1}H NMR (DMSO-d_6) δ 12.25 (s, 1H), 11.00 (s, 1H), 8.32 (s, 1H), 8.26 (d, J = 7.9 Hz, 1H), 7.90 (d, 1H), 7.71 (t, 1H), 6.31 (s, 1H), 1.88 (m, 1H), 0.92 (m, 2H), 0.62 (m, 2H); MS (EI) *m/z* (rel intensity) 295 (M^+, 15), 295 (15), 267 (21), 266 (10), 173 (99), 145 (99), 126 (13), 95 (18), 75 (15), 66 (19), 65 (18). Anal. ($C_{14}H_{12}F_3N_3O$) C, H, N.

***N*-(5-Cyclopropyl-1*H*-pyrazol-3-yl)-2-bromobenzamide (14):** yield 26%; mp 157−158 °C; ^{1}H NMR (DMSO-d_6) δ 12.15 (s, 1H), 10.75 (s, 1H), 7.65 (d, J = 7.7 Hz, 1H), 7.41 (app d, 1H), 7.35 (m, 2H), 6.26 (s, 1H), 1.86 (s, 1H), 0.919 (m, 2H), 0.677 (m, 2H); MS (FAB) *m/z* (rel intensity) 306 (MH^+, 99), 613 (10), 384 (15), 382 (15), 308 (97), 307 (26), 306 (99), 305 (13), 226 (10), 185 (15), 183 (16); HRMS (FAB) calcd for $C_{13}H_{12}BrN_3O$ + H1 306.0242, found 306.0250.

***N*-(5-Cyclopropyl-1*H*-pyrazol-3-yl)-2-chlorobenzamide (15):** yield 42%; mp 153−155 °C; ^{1}H NMR (DMSO-d_6) δ 12.15 (s, 1H), 10.75 (s, 1H), 7.47−7.37 (m, 4H), 6.25 (s, 1H), 1.87 (m, 1H), 0.916 (m, 2H), 0.675 (m, 2H); MS (EI) *m/z* (rel intensity) 261 (M^+, 6), 226 (22), 141 (23), 139 (99), 113 (19), 111 (58), 75 (42), 67 (17), 65 (38), 52 (16), 51 (24); HRMS (FAB) calcd for $C_{13}H_{12}ClN_3O$ + H1 262.0747, found 262.0737.

***N*-(5-Cyclopropyl-1*H*-pyrazol-3-yl)-2-methoxybenzamide (16):** yield 50%; ^{1}H NMR (DMSO-d_6) δ 12.14 (s, 1H), 10.70 (s, 1H), 7.51−7.35 (m, 4H), 6.24 (s, 1H), 3.69 (s, 3H), 1.86 (m, 1H), 0.92 (m, 2H), 0.66 (m, 2H); HRMS (FAB) calcd for $C_{14}H_{15}N_3O_2$ + H1 258.1237, found 258.1233.

***N*-(5-Cyclopropyl-1*H*-pyrazol-3-yl)-2,6-dichlorobenzamide (17):** yield 56%; ^{1}H NMR (DMSO-d_6) δ 12.17 (s, 1H), 10.72 (s, 1H), 7.55−7.34 (m, 3H), 6.26 (s, 1H), 1.88 (m, 1H), 0.93 (m, 2H), 0.68 (m, 2H); HRMS (FAB) calcd for $C_{13}H_{11}Cl_2N_3O$ + H1 296.0352, found 296.0348.

***N*-(5-Cyclopropyl-1*H*-pyrazol-3-yl)-3,4-dichlorobenzamide (18):** yield 42%; mp 195−196 °C; ^{1}H NMR (DMSO-d_6) δ 12.20 (s, 1H), 10.90 (s, 1H), 8.21 (s, 1H), 7.94 (d, J = 8.4 Hz, 1H), 7.76 (d, J = 8.4 Hz, 1H), 6.29 (s, 1H), 1.87 (m, 1H), 0.919 (m, 2H), 0.675 (m, 2H); HRMS (FAB) calcd for $C_{13}H_{11}Cl_2N_3O$ + H1 296.0357, found 296.0350.

***N*-(5-Cyclobutyl-1*H*-pyrazol-3-yl)-4-bromobenzamide (19):** yield 43%; mp 192−193 °C; ^{1}H NMR (DMSO-d_6) d 12.18 (s, 1H), 10.87 (s, 1H), 7.92 (d, J = 8.5 Hz, 2H), 7.63 (d, 2H), 6.28 (s, 1H), 2.65 (m, 1H), 2.08 (m, 2H), 1.94 (m, 2H), 1.65 (m, 2H); MS (EI) *m/z* (rel intensity) 319 (M^+, 5), 263 (59), 185 (96), 183 (99), 157 (76), 155 (82), 76 (83), 73 (74), 53 (56). Anal. ($C_{14}H_{14}BrN_3O$) C, H, N.

***N*-(5-Cyclopentyl-1*H*-pyrazol-3-yl)-4-bromobenzamide (20):** yield 62%; ^{1}H NMR (DMSO-d_6) δ 7.93 (d, J = 8.5 Hz, 2H), 7.65 (d, 2H), 6.32 (s, 1H), 2.51 (m, 1H), 2.22 (m, 4H), 1.82 (m, 2H), 1.41 (m, 2H); HRMS (FAB) calcd for $C_{15}H_{16}BrN_3O$ + H1 334.0549, found 334.0555.

***N*-(5-Cycloexyl-1*H*-pyrazol-3-yl)-4-bromobenzamide (21):** yield 60%; ^{1}H NMR (DMSO-d_6) δ 7.92 (d, J = 8.5 Hz, 2H), 7.61 (d, 2H), 6.29 (s, 1H), 2.38 (m, 1H), 1.96 (m, 2H), 1.66 (m, 2H), 1.26 (m, 6H); HRMS (FAB) calcd for $C_{16}H_{18}BrN_3O$ + H1 348.0706, found 348.0718.

***N*-(5-Methyl-1*H*-pyrazol-3-yl)-4-bromobenzamide (22):** yield 70%; mp 221−223 °C; ^{1}H NMR (DMSO-d_6) δ 2.10 (s, 1H), 10.80 (s, 1H), 7.90 (d, J = 9.0 Hz, 2H), 7.66 (d, J = 9.0 Hz, 2H), 6.37 (s, 1H), 2.20 (s, 3H). Anal. ($C_{11}H_{10}BrN_3O$) C, H, N.

***N*-(5-Ethyl-1*H*-pyrazol-3-yl)-4-bromobenzamide (23):** yield 27%; mp 253−254 °C; ^{1}H NMR (DMSO-d_6) δ 12.17 (s, 1H), 10.79 (s, 1H), 7.92 (d, J = 8.0 Hz, 2H), 7.69 (d, J = 8.0 Hz, 2H), 6.42 (s, 1H), 2.61 (q, J = 8 Hz, 2H), 1.20 (t, J = 8.0 Hz, 3H); HRMS (FAB) calcd for $C_{12}H_{12}BrN_3O$ + H1 294.0242, found 294.0247.

***N*-(5-Propyl-1*H*-pyrazol-3-yl)-4-bromobenzamide (24):** yield 67%; mp 186−187 °C; ^{1}H NMR (DMSO-d_6) δ 12.18 (s, 1H), 10.81 (s, 1H), 7.92 (d, J = 9.0 Hz, 2H), 7.69 (d, J = 8.0 Hz, 2H), 6.41 (s, 1H), 2.55 (t, 2H), 1.61 (m, 2H), 0.91 (t, J = 7.0 Hz, 3H); HRMS (FAB) calcd for $C_{13}H_{14}BrN_3O$ + H1 308.0399, found 308.0406, Anal. ($C_{13}H_{14}BrN_3O$) C, H, N.

***N*-(5-Isopropyl-1*H*-pyrazol-3-yl)-4-bromobenzamide (25):** yield 33%; mp 186−187 °C; ^{1}H NMR (DMSO-d_6) δ 12.16 (s, 1H), 10.81 (s, 1H), 7.90 (d, J = 9.0 Hz, 2H), 7.66 (d, J = 9.0 Hz, 2H), 6.39 (s, 1H), 2.91 (m, 1H), 1.21 (d, J = 7.0 Hz, 6H); HRMS (FAB) calcd for $C_{13}H_{14}BrN_3O$ + H1 308.0399, found 308.0398. Anal. ($C_{13}H_{14}BrN_3O$) C, H, N.

***N*-(5-*sec*-Butyl-1*H*-pyrazol-3-yl)-4-bromobenzamide (26):** yield 87%; ^{1}H NMR (DMSO-d_6) δ 12.19 (s, 1H), 10.87 (s, 1H), 7.92 (d, J = 7.0 Hz, 2H), 7.69 (d, J = 7.0 Hz, 2H), 6.40 (s, 1H), 2.71 (m, 1H), 1.57 (m, 2H), 1.21 (d, J = 7.0 Hz, 3H), 0.83 (t, 3H); MS (FAB) *m/z* (rel intensity) 322 (MH^+, 99), 183 (15), 139 (10), 89 (50); HRMS (FAB) calcd for $C_{14}H_{16}BrN_3O$ + H1 322.0555, found 322.0561.

***N*-(5-*tert*-Butyl-1*H*-pyrazol-3-yl)-4-bromobenzamide (27):** yield 88%; mp 241−243 °C; ^{1}H NMR (DMSO-d_6) δ 12.20 (s, 1H), 10.75 (s, 1H), 7.89 (d, J = 8.0 Hz, 2H), 7.67 (d, J = 8.0 Hz, 2H), 6.40 (s, 1H), 1.26 (s, 9H); HRMS (FAB) calcd for $C_{14}H_{16}BrN_3O$ + H1 322.0555, found 322.0561. Anal. ($C_{14}H_{16}BrN_3O$) C, H, N.

***N*-(5-Phenyl-1*H*-pyrazol-3-yl)-4-bromobenzamide (28):** yield 79%; mp 251−253 °C; ^{1}H NMR (DMSO-d_6) δ 12.97 (s, 1H), 10.95 (s, 1H), 7.95 (d, J = 8.0 Hz, 2H), 7.75−7.68 (m, 4H), 7.43 (t, 8H, 2H), 7.35 (t, J = 7.0 Hz, 1H), 7.03 (s, 1H); MS (EI) *m/z* (rel intensity) 341 (M^+, 10), 185 (98), 183 (99), 157 (47), 155 (50), 102 (63), 77 (44), 76 (67), 75 (42), 73 (76), 51 (32). Anal. ($C_{16}H_{12}BrN_3O$) C, H, N.

***N*-(5-Benzyl-1*H*-pyrazol-3-yl)-4-bromobenzamide (29):** yield 36%; mp 185−187 °C; ^{1}H NMR (DMSO-d_6) δ 7.88 (d, J = 8.0 Hz, 2H), 7.65 (d, J = 8.0 Hz, 2H), 7.27 (m, 5H), 6.32 (s, 1H), 3.91 (s, 2H); HRMS (FAB) calcd for $C_{17}H_{14}BrN_3O$ + H1 356.0399, found 356.0402. Anal. ($C_{17}H_{14}BrN_3O$) C, H, N.

Methyl 4-{[(5-cyclopropyl-1*H*-pyrazol-3-yl)amino]-carbonyl}benzoate (43): yield 40%; mp 172−174 °C; ^{1}H NMR (DMSO-d_6) δ 12.20 (s, 1H), 10.90 (s, 1H), 8.06 (d, J = 8.0 Hz, 2H), 8.01 (d, J = 8.0 Hz, 2H), 6.30 (s, 1H), 3.87 (s, 3H), 1.88 (m, 1H) 0.91 (m, 2H), 0.67 (m, 2H); MS (EI) *m/z* (rel intensity) 285 (M^+, 9), 256 (13), 163 (99), 136 (21), 135 (22), 119 (14), 104 (14), 103 (28), 77 (15), 75 (18); HRMS (FAB) calcd for $C_{15}H_{15}N_3O_3$ + H1 286.1191, found 286.1194.

Method B. 2-(1,1′-Biphenyl-4-yl)-*N*−(5-cyclopropyl-1*H*-pyrazol-3-yl)acetamide (35). To a solution of 45.6 mg (0.215 mmol) of 1,1′-biphenyl-4-ylacetic acid in 3 mL of dichloromethane at 0 °C, 41.2 mg (0.215 mmol) of *N*-(3-dimethylaminopropyl)-*N*′-ethylcarbodiimide hydrochloride was added. After 1 h at the same temperature under stirring, 40 mg (0.179 mmol) of *tert*-butyl-3-amino-5-cyclopropyl-1*H*-pyrazole-1-carboxylate was added. The mixture was maintained at room temperature for 16 h, then was diluted with dichloromethane and washed with a saturated solution of sodium hydrogenocarbonate. The organic layer was dried over anhydrous sodium sulfate and evaporated to dryness to give after column chromatography (hexanes/ethyl acetate) 60 mg (80% yield) of 2-(1,1′-biphenyl-4-yl)-*N*-(5-cyclopropyl-l-terbutoxycarbonylpyrazol-3-yl)acetamide. This intermediate was submitted to hydrolysis with 15 mL of trifluoroacetic acid, 10% v/v, in dichloromethane for 1 h. The solvent was then evaporated under vacuum. The residue redissolved with dichloromethane and was washed with a saturated solution of sodium hydrogen carbonate. The organic layer was dried over anhydrous sodium sulfate and evaporated to give 42 mg (92% yield) of the title compound. ^{1}H NMR (DMSO-d_6) δ 7.6−7.3 (m, 9H), 6.09 (s, 1H), 3.59 (s, 2H), 1.81 (m, 1H); ESI(+) MS *m/z* 318 (100, MH^+); HRMS (FAB) calcd for $C_{20}H_{19}N_3O$ + H1 318.1601, found 318.1605. Anal. ($C_{20}H_{19}N_3O$) C, H, N.

Analogously, by use of *tert*-butyl 3-amino-5-cyclopropyl-1*H*-pyrazole-1-carboxylate and a suitable carboxylic acid, the following compounds were prepared.

***N*-(3-Cyclopropyl-1*H*-pyrazol-5-yl)phenylacetamide (30):** yield 65%); mp 206−208 °C; ^{1}H NMR (DMSO-d_6) δ 12.05 (s, 1H), 10.5 (s, 1H), 7.28 (app d, 4H), 7.21 (m, 1H), 6.10 (s, 1H), 3.54 (s, 2H), 1.80 (m, 2H), 0.59 (m, 2H); MS (EI) *m/z* (rel intensity) 241 (M^+, 64), 123 (99), 118 (10), 96 (16), 95 (9), 91 (99), 80 (35), 73 (14), 66 (10), 65 (48). Anal. ($C_{14}H_{15}N_3O$) C, H, N.

4-{2-[(3-Cyclopropyl-1*H*-pyrazol-5-yl)amino]-2-oxoethyl}benzamide (31): yield 71%; mp >250 °C; ^{1}H NMR (DMSO-d_6) δ 10.45 (s, 1H), 7.77 (dd, J = 6.5, 1.8 Hz, 2H), 6.09 (s, 1H), 3.61 (s, 2H), 1.81 (m, 1H); HRMS (FAB) calcd for $C_{15}H_{16}N_4O_2$ + H1 285.1346, found 285.1346. ESI(+) MS *m/z* 285 (100, MH^+). Anal. ($C_{15}H_{16}N_4O_2$) C (calcd 63.37, found 61.28), H, N (calcd 19.71, found 18.52).

***N*-(3-Cyclopropyl-1*H*-pyrazol-5-yl)-2-(3-methoxyphenyl)-acetamide (32):** yield 78%); mp 186−188 °C; ^{1}H NMR (DMSO-d_6) δ 12.03 (s, 1H), 10.41 (s, 1H), 6.80−7.23 (3m, 4H), 6.13 (s, 1H), 3.75 (s, 3H), 3.54 (s, 2H), 1.84 (m, 1H), 0.91 (m, 2H), 0.63 (m, 2H); MS (ESI+) *m/z* (rel intensity) 565 ($2MNa^+$, 20), 272 (MH^+, 100), 254 (10). Anal. ($C_{15}H_{17}N_3O_2$) C, H, N.

***N*-(3-Cyclopropyl-1*H*-pyrazol-5-yl)-2-[4-(2-pyrrolidin-1-ylethoxy)phenyl]acetamide (33):** yield 80%; ^{1}H NMR (400 MHz, DMSO-d_6) δ 11.92 (s, 1H), 10.34 (s, 1H), 7.19 (d, J = 8.7 Hz, 2H), 6.85 (d, J = 8.7 Hz, 2H), 6.07 (s, 1H), 4.02 (t, J = 5.8 Hz, 2H), 3.46 (s, 2H), 2.83 (t, J = 7.3 Hz, 2H), 2.58 (s, 4H), 1.81 (tt, J = 8.5 and 5.0 Hz, 1H), 1.67 (dt, J = 6.3 and 3.3 Hz, 4H), 0.88 (ddd, J = 8.4, 6.4, and 4.1 Hz, 2H), 0.60 (ddd, J = 6.4, 5.0, and 4.2 Hz, 2H); MS (ESI+) *m/z* (rel intensity) 731 ($2MNa^+$, 20), 377 (MNa^+, 8), 355 (MH^+, 100); HRMS (FAB) calcd for $C_{20}H_{26}N_4O_2$ + H1 355.2128, found 355.2133.

***N*-(3-Cyclopropyl-1*H*-pyrazol-5-yl)-2-(4-trifluoromethoxyphenyl)acetamide (34):** yield 78%; ^{1}H NMR (DMSO-d_6) δ 10.48 (s, 1H), 7.4−7.2 (m, 4H), 6.08 (s, 1H), 3.60 (s, 2H), 1.81 (m, 1H); ESI(+) MS: *m/z* 326 (100, MH^+); HRMS (FAB) calcd for $C_{15}H_{14}F_3N_3O_2$ + H1 326.1111, found 326.1116.

***N*-(3-Cyclopropyl-1*H*-pyrazol-5-yl)-2-(3′-fluoro[1,1′-biphenyl]-4-yl)acetamide (36):** yield 75%; ^{1}H NMR (400 MHz, DMSO-d_6) δ 10.49 (s, 1H), 7.63 (d, J = 8.2 Hz, 2H), 7.38 (d, J = 8.2 Hz, 2H), 6.09 (s, 1H), 3.59 (s, 2H), 1.82 (m, 1H); MS (ESI+) *m/z* (rel intensity) 693 ($2MNa^+$, 15), 358 (MNa^+, 8), 336 (MH^+, 100), 185 (22); HRMS (FAB) calcd for $C_{20}H_{18}FN_3O$ + H1 336.1507, found 336.1512.

***N*-(3-Cyclopropyl-1*H*-pyrazol-5-yl)-2-(3′-methyl[1,1′-biphenyl]-4-yl)acetamide (37):** yield 79%); ^{1}H NMR (400 MHz, DMSO-d_6) δ 11.99 (s, 1H), 10.46 (s, 1H), 7.13−7.57 (m, 8H), 6.09 (s, 1H), 3.59 (s, 2H), 2.35 (s, 3H), 1.81 (tt, J = 8.4 and 5.1 Hz, 1H), 0.88 (ddd, J = 8.4, 6.4, and 4.1 Hz, 2H), 0.61 (ddd, J = 6.4, 5.1, and 4.1 Hz, 2H); MS (ESI+) *m/z* (rel intensity) 685 ($2MNa^+$, 15), 332 (MH^+, 100), 181 (35); HRMS (FAB) calcd for $C_{21}H_{21}N_3O$ + H1 332.1757, found 332.1761.

***N*-(5-Cyclopropyl-1*H*-pyrazol-3-yl)-2-(4-thien-2-yl-phenyl)acetamide (40):** yield 75%); ^{1}H NMR (400 MHz, DMSO-d_6) δ 10.47 (s, 1H), 7.6−7.1 (m, 7H), 6.08 (s, 1H), 1.82 (m, 1H); ESI(+) MS *m/z* 324 (100, MH^+); HRMS (FAB) calcd for $C_{18}H_{17}N_3OS$ + H1 324.1165, found 324.1173.

***N*-(5-Cyclopropyl-1*H*-pyrazol-3-yl)-2-(2-naphthyl)-acetamide (41):** yield 82%; ^{1}H NMR (DMSO-d_6) δ 6.10 (s, 1H), 3.73 (s, 2H), 1.80 (m, 1H); ESI(+) MS *m/z* 292 (100, MH^+); ^{13}C NMR (DMSO-d_6) δ 7.2 (CH-6), 8.1 (CH2−7,CH2−8), 43.1 (CH2−12), 92.8 (CH-4), 126.0, 126.5 (CH19,CH-18), 127.8, 127.9, 128.0, 128.1 (CH-14, CH-22, CH-15, CH-20, CH-17), 132.3, 133.4 (C-16, C-21), 134.4 (C-13), 145.8 (C-3), 147.8 (C-5) 168.4 (C-10); HRMS (FAB) calcd for $C_{18}H_{17}N_3O$ + H1 292.1444, found 292.1452. Anal. ($C_{18}H_{17}N_3O$) C, H, N.

***N*-(5-Cyclopropyl-1*H*-pyrazol-3-yl)-2-(1-naphthyl)-acetamide (42):** yield 78%); ^{1}H NMR (400 MHz, DMSO-d_6) δ 6.07 (s, 1H), 4.07 (s, 2H), 1.80 (m, 1H); ESI (+) MS *m/z* 292 (100, MH+); HRMS (FAB) calcd for $C_{18}H_{17}N_3O$ + H1 292.1444, found 292.1452.

Methyl 4′-{2-[(5-cyclopropyl-1*H*-pyrazol-3-yl)amino]-2-oxoethyl}-1,1′-biphenyl-4-carboxylate (44): yield 74%; ^{1}H NMR (DMSO-d_6) δ 7.9−7.3 (m, 8H), 6.11 (s, 1H), 3.58 (s, 2H), 1.85 (m, 1H); ESI(+) MS *m/z* 376 (100, MH^+); HRMS (FAB) calcd for $C_{22}H_{21}N_3O_3$ + H1 376.1656, found 376.1651

Methyl [4-(2-Chloroethoxy)phenyl]acetate (45). A mixture of methyl (*p*-hydroxyphenyl)acetate (30 g, 0.18 mol), 1-bromo-2-chloroethane (15 mL, 0.18 mol), and anhydrous potassium carbonate (37 g) in anhydrous acetone (200 mL) was refluxed. An equivalent amount of 1-bromo-2-chloroethane was added three more times at intervals of 40 h. After the mixture was cooled, the precipitate was filtered off and the solution was evaporated. The residue was taken up with ether (1 L), the suspension obtained was filtered, and the solution was washed with 1 N NaOH (200 mL, then 100 mL) and brine. The organic layer was evaporated to dryness to give the phenylacetate derivative as an oily semisolid (29 g, 70% yield). ^{1}H NMR ($CDCl_3$) δ 3.6 (2H, s), 3.7 (3H, s), 3.8 (2H, t), 4.2 (2H, t), 6.9 (2H, m), 7.2 (2H, m).

Methyl [4-(2-Pyrrolidin-1-ylethoxy)phenyl]acetate (46). A mixture of methyl [4-(2-chloroethoxy)phenyl]acetate (10.0 g, 44 mmol), pirrolidine (18 mL, 220 mmol), and potassium iodide (3.6 g, 22 mmol) in anhydrous dimethylformamide (55 mL) was heated at 100 °C for 5 h. The solution was acidified and extracted with ether to eliminate unreacted products. Then the solution was basified (pH ∼8) and extracted with chloroform. The organic solution was washed with brine, and the solvent was evaporated to dryness. The residue was purified by flash chromatography with dichloromethane/methanol/30% NH_4OH aqueous (95:5:0.5). The product was obtained in 48% yield (5.5 g). ^{1}H NMR ($CDCl_3$) δ 1.8 (4H, m), 2.6 (4H, m), 2.9 (2H, t), 3.55 (2H, s), 3.7 (3H, s), 4.1 (2H, t), 6.9 (2H, m), 7.2 (2H, m).

[4-(2-Pyrrolidin-1-ylethoxy)phenyl]acetic Acid (47). A mixture of methyl [4-(2-pyrrolidin-1-ylethoxy)phenyl]acetate (4.3 g, 16 mmol) and a solution of 1 N sodium hydroxide (17 mL) was stirred at room temperature for 24 h. The basic solution was extracted with dichloromethane/MeOH (90:10), neutralized with 1 N HCl (17 mL), and then evaporated to dryness. The residue was taken up with chloroform, the suspension obtained was filtered, and the solution was evaporated to afford an oil that solidified on standing. This solid was triturated in ether to give the acid as a beige hygroscopic powder (3.5 g, 86%): mp 96−98 °C; ^{1}H NMR ($CDCl_3$) δ 1.7 (4H, m), 2.55 (4H, m), 2.8 (2H, t), 3.45 (2H, s), 4.0 (2H, t), 6.85 (2H, m), 7.15 (2H, m). Anal. ($C_{14}H_{19}NO_3$) C (calcd 67.45, found 64.13), H, N.

4-{[(5-Cyclopropyl-1*H*-pyrazol-3-yl)amino]carbonyl}-benzoic Acid (8). To a solution of 80 mg (0.28 mmol) of **43** in 5 mL of methanol, 2.5 mL of water, 2.5 mL of THF, and 80 mg (1.43 mmol) of KOH were added. After 2 hours under stirring at room temperature, the organic solvent was removed, and the product was precipitated with 10% HCl, giving 40 mg (50% yield) of **8** as a white solid (50%): mp 291−293 °C; ^{1}H NMR (DMSO-d_6) δ 12.70 (bs, 1H), 10.90 (s, 1H), 8.03 (d, J = 8.0 Hz, 2H), 7.99 (d, J = 8.0 Hz, 2H), 6.28 (s, 1H), 1.88 (m, 1H), 0.91 (m, 2H), 0.67 (m, 2H); HRMS (FAB) calcd for $C_{14}H_{13}N_3O_3$ + H1 272.1035, found 272.1030.

Analogously, by use of compound **44**, compound **38** was obtained.

4′-{2-[(5-Cyclopropyl-1*H*-pyrazol-3-yl)amino]-2-oxoethyl}-1,1′-biphenyl-4-carboxylic acid (38): yield 58%; ^{1}H NMR (400 MHz, DMSO-d_6) δ 10.46 (s, 1H), 6.09 (s, 1H), 3.61 (s, 2H), 1.81 (m, 1H); ESI (+) MS *m/z* 362 (100, MH+); HRMS (FAB) calcd for $C_{21}H_{19}N_3O_3$ + H1 362.1499, found 362.1487.

***N*-(5-Cyclopropyl-1*H*-pyrazol-3-yl)terephthalamide (9).** To **43** (0.12 g, 0.42 mmol) was added 20 mL of aqueous (30%) ammonium hydroxyde, and the heterogeneous mixture was vigorously stirred overnight, loosely stoppered. The resulting solid was filtered and washed with water to remove ammonia and then with ethyl acetate to remove residual ester. The solid was dissolved in warm methanol and concentrated to afford 65 mg of **9** as a white powder (57%): mp 261−263 °C; ^{1}H NMR (DMSO-d_6) δ 12.20 (s, 1H), 10.85 (s, 1H), 8.09 (s, 1H), 8.01 (d, J = 8.0 Hz, 2H), 7.92 (d, J = 8.0 Hz, 2H), 7.50 (s, 1H), 6.28 (s, 1H), 1.87 (m, 1H), 0.91 (m, 2H), 0.67 (m, 2H); MS (EI) *m/z* (rel intensity) 270 (M^+, 10), 148 (99), 128 (72), 103 (25), 73 (40), 71 (42), 60 (25), 59 (58), 58 (50); HRMS (FAB) calcd for $C_{14}H_{14}N_4O_2$ + H1 271.1195, found 271.1197.

Analogously, by use of compound **44**, compound **39** was obtained.

4′-{2-[(5-Cyclopropyl-1*H*-pyrazol-3-yl)amino]-2-oxoethyl}-1,1′-biphenyl-4-carboxamide (39): yield 61%; ^{1}H NMR (400 MHz, DMSO-d_6) δ 10.46 (s, 1H), 6.09 (s, 1H), 3.61 (s, 2H), 1.81 (m, 1H); ESI(+) MS *m/z* 361 (100, MH^+); HRMS (FAB) calcd for $C_{21}H_{20}N_4O_2$ + H1 361.1659, found 361.1662.

II. Registry Numbers (RN). Benzoyl chloride (RN, 98-88-4); butyryl chloride (RN, 141-75-3); 4-bromobenzoyl chloride (RN, 586-75-4); 4-chlorobenzoyl chloride (RN, 122-01-0); 4-methoxybenzoyl chloride (RN, 100-07-2); 4-chlorocarbonylbenzoic acid methyl ester (RN, 7377-26-6); 3-bromobenzoyl chloride (RN, 1711-09-7); 3-chlorobenzoyl chloride (618-46-2); 3-methoxybenzoyl chloride (RN, 1711-05-3); 3-trifluoromethylbenzoyl chloride (RN, 2251-65-2); 2-bromobenzoyl chloride (RN, 7154-66-7); 2-chlorobenzoyl chloride (RN, 609-65-4); 2-methoxybenzoyl chloride (21615-34-9); 2,6-dichlorobenzoyl chloride (RN, 4659-45-4); 3,4-dichlorobenzoyl chloride (3024-72-4); phenylacetic acid (RN, 103-82-2); (4-carbamoylphenyl)acetic acid (RN, 2393-28-4); (3-methoxyphenyl)acetic acid (RN, 1798-09-0); (4-trifluoromethoxyphenyl)acetic acid (RN, 4315-07-5); biphenyl-4-ylacetic acid (RN, 5728-52-9); (3′-fluorobiphenyl-4-yl)acetic acid (RN, 5002-38-0); (3′-methylbiphenyl-4-yl)acetic acid (RN, 296777-83-8), 4′-carboxymethylbiphenyl-4-carboxylic acid methyl ester (RN, 540467-44-5), (4-thiophen-2-yl-phenyl)acetic acid (RN, 252561-11-8); naphthalen-2-ylacetic acid (RN, 581-96-4); naphthalen-1-ylacetic acid (RN, 86-87-3); 5-methyl-3-amino-1*H*-pyrazole (RN, 31230-17-8); 5-cyclopropyl-3-amino-1*H*-pyrazole (RN, 175137-46-9); 5-cyclobutyl-3-amino-1*H*-pyrazole (RN, 326827-21-8); 5-cyclopentyl-3-amino-1*H*-pyrazole (RN, 264209-16-7); 5-cyclohexyl-3-amino-1*H*-pyrazole (RN, 81542-54-3); ethyl-3-amino-1*H*-pyrazole (RN, 1924-24-1); 5-propyl-3-amino-1*H*-pyrazole (RN, 56367-26-1); 5-isopropyl-3-amino-1*H*-pyrazole (RN, 56367-24-9); 5-*sec*-butyl-3-amino-1*H*-pyrazole (RN, 56367-25-0); 5-*tert*-butyl-3-amino-1*H*-pyrazole (RN, 82560-12-1); 5-phenyl-3-amino-1*H*-pyrazole (RN, 1572-10-7); 5-benzyl-3-amino-1*H*-pyrazole (RN, 150712-24-6).

III. Kinase Assays. The biochemical activity of compounds was determined by incubation with specific enzymes and substrates, followed by quantitation of the phosphorylated product. Compounds were 3-fold serially diluted from 10 to 0.0015 μM, then incubated for 30−90 min at room temperature

in the presence of ATP/$P^{33}\gamma$-ATP mix [$2K_m$], substrate [$5K_m$], and the specific enzyme [0.7−100 nM] in a final volume of 30 μL of kinase buffer, using 96 U bottom plates. The final concentration of DMSO was 1%.

A summary of kinase assay conditions follows.

buffer A: Tris-HCl, pH 7.4, 10 mM; $MgCl_2$, 10 mM; DTT 7.4 mM.

buffer B: Hepes, pH 7.5, 50 mM; $MgCl_2$, 3 mM; $MnCl_2$, 3 mM; DTT, 1 mM; $NaVO_3$, 3 μM.

buffer C: Hepes, pH 7.5, 50 mM; $MgCl_2$ 5 mM; DTT, 1 mM; $NaVO_3$, 3 μM.

buffer D: Hepes, pH 7.5, 50 mM; $MnCl_2$ 3 mM; DTT, 1 mM; $NaVO_3$, 3 μM.

buffer E: Mops, pH 6.8, 50 mM; $MgCl_2$, 10 mM; DTT, 1 mM; $NaVO_3$, 3 μM.

After incubation, the reaction was stopped and the phosphorylated substrate was separated from nonincorporated radioactive ATP using SPA beads (Amersham Pharmacia Biotech), Dowex resin (Supelco), or Multiscreen phosphocellulose filter (Millipore) as described below.

III.1. SPA Assays. The reaction was stopped by the addition of 100 μL of PBS + 32 mM EDTA + 0.1% Triton X-100 + 500 μM ATP, containing 1 mg of streptavidin-coated SPA beads (biotin capacity 130 pmol/mg). After 20 min of incubation for substrate capture, 100 μL of the reaction mixture was transferred into Optiplate (PerkinElmer) 96-well plates containing 100 μL of 5 M CsCl, left to stand for 4 h to allow stratification of beads to the top of the plate, and counted using TopCount (Packard) to measure substrate-incorporated phosphate.

III.2. Dowex Resin Assay. An amount of 150 μL of resin/formate, pH 3.00, was added to stop the reaction and capture unreacted $P^{33}\gamma$-ATP, separating it from the phosphorylated substrate in solution. After 60 min of rest, a volume of 50 μL of supernatant was transferred to Optiplate 96-well plates. After the additon of 150 μL of Microscint 40 (Packard), the radioactivity was counted in the TopCount.

III.3. Multiscreen Assay. The reaction was stopped with the addition of 10 μL of EDTA, 150 mM. An amount of 100 μL was transferred to a MultiScreen plate to allow substrate binding to phosphocellulose filter. Plates were then washed three times with 100 μL of H_2PO_4, 75 mM, filtered by a MultiScreen filtration system, and dried. After the additon of 100 μL of Microscint 0 (Packard), radioactivity was counted in the TopCount.

Experimental data were analyzed by the computer program Assay Explorer (MDL Information System) using the four-parameter logistic equation

$$y = \text{bottom} + \frac{\text{top} - \text{bottom}}{1 + 10^{[\log(IC_{50}) - x]\text{slope}}}$$

where x is the logarithm of the inhibitor concentration and y is the response; y starts at bottom and goes to the top with a sigmoid shape.

At least two independent experiments were performed for each compound in order to determine IC_{50} in replicates, and potency is expressed by the mean of IC_{50} values obtained by nonlinear regression analysis. Coefficient of variance (SD/mean) ranges from 10% to 24%. Staurosporine (Sigma) was included as standard in all kinase assays except for p38α kinase, for which SB203580 (Calbiochem) was used. All kinases were produced in house as recombinant proteins expressed in insect cells (except for CK2, PKCbeta, and LYN, which were purchased from Upstate). A detailed description of the assay panel production and characterization will be published elsewhere.[32] Substrate peptides were purchased from Primm (AKTide, CHOCKtide4X, CHKtide, IRStide, Gastrin) and from American peptides (IKBalpha). MBP, histone H1, and alphaCasein proteins were purchased from Sigma. KITtide, PDKtide, PAKtide, MCM2, and RB substrates were produced in our laboratories. Protein biotinylation required for SPA assay format was performed in house.

IV. Production of CDK2/Cyclin A Complex. Expression and Purification of Cyclin A. A cDNA encoding residues 173−432 of human cyclin A was amplified by the polymerase chain reaction (PCR) and cloned into the N-terminal GST fusion bacterial expression vector, pGEX6P (Amersham). GST-cyclinA was expressed in the *E. coli* host strain BL21trx (Novagen). Cell cultures were grown in LB media to an optical density of 0.8 at 25 °C and induced with 0.1 mM IPTG. Growth was continued overnight at 25 °C. Cells were harvested by low-speed centrifugation and lysed by passage through a APV homogenizer (50 mM Tris, pH 7.9, 150 mM NaCl, 20 mM DTT). The soluble fraction was applied to glutathione sepharose resin (Amersham), and the GST moiety was removed, after extensive washes, by cleavage with PreScission Protease (Amersham). The resulting cyclin A in solution was estimated to be 95% pure by SDS−PAGE.

IV.1. Expression and Purification of CDK2. A human cDNA clone encoding full-length CDK2 was amplified by PCR and cloned into a pVL1392 vector (Pharmingen) for expression in HighFive (Invitrogen) insect cells as a GST fusion. Infection with virus was done at a Moi of 1 for 48 h at 27 °C. Cells were harvested and lysed by APV homogenizer in the same buffer as above. The supernatant was loaded onto a glutathione sepharose (Pharmacia) column and washed with buffer (DPBS, Sigma).

IV.2. CDK2/Cyclin A Complex Formation and Purification. The resulting resin, with GST-CDK2 linked, was incubated for 1 h at 4 °C with the previously purified cyclin A. After extensive washes and cleavage with PreScission protease, the complex CDK2/cyclin A, pure at 99% (SDS−PAGE and gel filtration), was obtained. A final gel filtration on a Superdex 200 column (Amersham) allowed us to obtain the complex with no detectable impurities in the final buffer, 40 mM HEPES, pH 7.0, 200 mM NaCl, 5 mM DTT.

V. Crystal Structure of CDK2/Cyclin A with Compound 41. Following purification, the protein was concentrated to 10 mg/mL in a buffer containing 40 mM Hepes, pH 7.0, 0.2 M NaCl, and 5 mM DTT. Crystals of CDK2/cyclin A were grown at 4 °C by the hanging drop method essentially as described by Jeffrey et al.[34] An amount of 2 μL of the protein solution was mixed with an equal volume of well solution containing 20% saturated ammonium sulfate, 1 M KCl, 40 mM Hepes, pH 7.0. The drops were streak-seeded 1 day later, and large crystals grew after a further 1 day period. For soaking of the compound into the crystal, a crystal was transferred to a solution containing 50% saturated ammonium sulfate, 0.4 M KCl, 40 mM Hepes, pH 7.0, 20% glycerol, and compound **41** at a concentration of approximately 4 mM (the compound did not dissolve completely). Data were collected as described in Table 7 and processed using the HKL suite of programs.[35] The starting model for the refinement was a structure based on the structure of 1FIN[34] that had been subject to some refinement at 2.2 Å against data collected as described here but with another compound. Refinement was carried out in CNX.[36] The structure has been deposited in the Protein Data Bank (PDB) with the code 1VYZ.

VI. Crystal Structure of CDK2 with Compound 4. The CDK2 protein was produced and purified following the published protocol.[37] Crystals of the apoprotein were grown at 20 °C by the hanging drop vapor diffusion method as previously reported[38] but using a protein concentration of 3 mg/mL. To make the soak solution, compound **4** was first dissolved in DMSO at a concentration of 50 mM. An amount of 15 μL of this DMSO stock solution was then added to 85 μL of a solution containing 15% PEG3350, 50 mM ammonium acetate, and 0.1 M Hepes, pH 7.4. Crystals were soaked for 9 h and then transferred to the cryoprotectant solution (10% PEG3350, 50 mM ammonium acetate, 0.1 M Hepes, pH 7.4, 25% glycerol). X-ray data were collected at the ESRF beamline ID14-4 (Grenoble, France). Data were processed using the HKL suite[35] and refined using the program CNX.[36] The crystallographic data are summarized in Table 7 (PDB 1VYZ).

Table 7. Crystallographic Data for **4** and **41**

	CDK2 with **4**	CDK2/cyclin A with **41**
Data Collection		
X-ray source	ESRF ID14-4	ESRF ID14-2
space group	$P2_12_12_1$	$P6_222$
a (Å)	53.3	184.2
b (Å)	71.9	184.2
c (Å)	72.22	214.7
α (deg)	90.0	90.0
β (deg)	90.0	90.0
γ (deg)	90.0	120.0
resoln (Å)	30−2.2 (2.28−2.0)[a]	35−2.3 (2.38−2.3)[a]
no. of measd reflns	71 050	456 814
no. of unique reflns	14 353	94 577
completeness (%)	99.5 (99.6)	99.4 (97.1)
$I/\sigma(I)$	14.0(3.3)	16(2.3)
R_{merge} (%)	0.048 (0.389)	0.081 (0.69)
Refinement		
R_{factor} (%)	24.4	23.0
R_{free} (%)	30.5	25.9
no. of protein atoms	2246	8978
no. of nonprotein atoms	79	450
rmsd from ideal values		
bond (Å)	0.012	0.007
angles (deg)	1.53	1.26
rmsd B values of bonded atoms	2.4	1.6
% of residues in disallowed regions of Ramachandran plot[b] (%)	1.5	1.6
av B value (protein)	39.5	54
av B value (inhibitor)	30.9	45

[a] Values in parentheses are for the highest-resolution shells. [b] As defined by Kleywegt and Jones.[39]

VII. In Vitro Pharmacokinetics. VII.1. High-Throughput Solubility. The method for estimating nonequilibrium solubility was based on turbidity detection in 96-well microtiter plates. Small aliquots of high concentration DMSO stock solution were diluted into buffer, and turbidity was detected using plate readers. Solubility was reported as an average from the highest concentration without turbidity to the lowest concentration with turbidity. Typically utilized were 10 mM DMSO stocks and measured turbidity at 50 and 250 μM (with 2.5% DMSO) in pH 3, 7, and 10 buffers.

VII.2. Cell Permeability. Caco2 cells were grown on microporous membrane support, the monolayers were inserted into multi-trans-well plates, which allowed measurements of permeability in both apical to basolateral and basolateral to apical directions. Transport experiments were performed using the Multiprobe II Plus (Packard) and 12-well plates or 24-trans-well plates, which were placed on a heated plate shaker to provide the right temperature and agitation rate. Test compounds were determined by LC/MS/MS in the two chambers prior to and 120 min after incubation (10 μM).

VII.3. Plasma Protein Binding. Plasma protein binding was determined by evaluating HPLC retention with a human serum albumin (HSA) coupled column. The percentage was determined by comparing the retention time of the test compound to those of known standards.

VII.4. Metabolic Stability (Rat Hepatocytes). The compound was incubated at 37 °C in 24-well plates under continuous shaking at a concentration of 1 μM in the presence of 10^6 rat hepatocytes in a final volume of 1 mL of Leibovitz's medium. From the same well at different time points (0.5, 10, 20, 30, 40, 60, and 90 min), 75 μL of incubation medium was taken and transferred into a 96-well plate containing in each well 75 μL of ice-cold acetonitrile to stop the reaction. At the same time, control incubations in Leibovitz's medium (absence of hepatocytes) were performed to determine the stability of the compound during the incubation time. After centrifuging the 96-well plates, the supernatant was directly injected into an LC/MS/MS system and the amount of parent was measured. Typical low, moderate, and high clearance drugs were included in the assay as reference compounds.

VIII. In Vivo Pharmacokinetics. The pharmacokinetics was investigated in male Sprague Dawley rats that fasted overnight, following a single dose given intravenously (iv) or orally (os). The vehicle used was PEG400, 4% Tween 80/dextrose (60:40). A total of six rats were used (three for each leg). Plasma samples were collected from each rat from the jugular vein. Blood samples were collected at predose at 5, 15, and 30 min and 1, 2, 4, 6, and 24 h after dosing. The mean body weight of the rats was approximately 270. Blood samples were collected into heparinized syringes from the venous catheter and transferred immediately into precooled tubes placed in an ice/water bath. The samples were centrifuged at 10000g for 3 min at 4 °C. Plasma samples were placed in precooled tubes and frozen at −80 °C until until analysis. Samples were analyzed by LC/MS/MS. The pharmacokinetic parameters were derived by noncompartmental methods using the WinNonLin software program. The C_{max} and T_{max} values were recorded directly from experimental observations. The AUC_{tot} values were calculated using a linear trapezoidal rule. The total body clearance (Cl), MRT, and the steady-state volume of distribution (V_{ss}) were also calculated after iv administration. The oral bioavailability (expressed as percent) was estimated by taking the ratio of dose-normalized AUC values after oral doses to those after iv doses

IX. Cell Culture. HCT-116 and HT-29 human colon carcinoma cells were grown in McCoy's medium supplemented with 10% FCS. A2780 human ovarian carcinoma and DU-145 human prostate carcinoma cells were grown in RPMI-1640 medium supplemented with 10% FCS.

X. Inhibition of Cell Proliferation. Exponentially growing cells were seeded in 96-well plates (10 000 cells/cm^2 for A2780 and HT-29; 5000 cells/cm^2 for HCT-116 and DU-145) and incubated at 37 °C in a humidified 5% CO_2 atmosphere. After 24 h, scalar concentrations of test compounds were added for 72 h. At the end of the treatment, cell proliferation was determined by the SRB assay.[33] The 50% inhibitory concentration (IC_{50}) was calculated on the derived concentration−response curve (four replicates of two experiments for each data point).

XI. Cell Treatment after Synchronization with Nocodazole. Twenty-four hours after seeding, HT-29 cells were treated with nocodazole (Sigma, St. Louis, MO) at a final concentration of 75 ng/mL and incubated at 37 °C and 5% CO_2 for 20 h.

After "mitotic shake-off", only nonadherent (synchronized) cells were collected, washed with PBS, and seeded in complete medium at a concentration of 1×10^5 cells/mL and some of them were immediately treated with **41** for 16 h.

Thirty minutes before the end of treatment, cells were pulsed with BrdU (10 μM final concentration) and then collected by trypsinization and washed with PBS.

XII. DNA Content Determination. Cells were fixed in ice-cold 70% ethanol (1 mL/10^6 cells) and maintained at −20 °C for at least 12 h.

After centrifugation (200g for 5 min), cell pellet was washed with PBS and then stained with 1 mL of a solution of propidium iodide (Sigma, St. Louis, MO), 50 μg/mL in sodium citrate (0.1%) + 12.5 μL of RNAse (Sigma, St. Louis, MO) (0.5 mg/mL), and 12.5 μL of NONIDET P40 (Amresco, Solon, OHIO) (0.1%).

After incubation for 1 h at room temperature in the dark, cytofluorimetric analysis was performed using a FACScan (Becton Dickinson, San Jose,CA).

XIII. Western Blot Analysis. Western blotting was performed using whole-cell protein extracts obtained by precipitation with trichloroacetic acid (TCA). The protein content was measured with a BCA protein assay kit (Pierce). An amount of 20 μg of protein samples was separated on 7.5% SDS−PAGE gel and transferred to nitrocellulose membranes (Hybond ECL, Amersham). The membranes were blocked with 5% milk in TBS/0.1% Tween 20 for 1 h and subsequently probed with primary antibody (antihuman Rb clone G3-245, Pharmingen)

overnight at 4 °C and then with horseradish peroxidase (HRP) conjugated secondary antibody (goat anti-mouse IgG(H+L), Pierce) for 1 h at room temperature. The protein bands were visualized with a chemiluminescent assay system (SupersignalWest Pico, Pierce).

XIV. Microscopic Analysis of BrdU Incorporation. The staining was performed on cytocentrifuged slides of the labeled cells fixed in cold acetone for 10 min and air-dried. To denature the DNA and produce single-stranded molecules, the slides were immerse in 2 N HCl/Triton X-100 for 10 min and then in PBS to neutralize the acid. Anti-BrdU FITC conjugated antibody (Becton Dickinson) diluted in 0.5% Tween 20/PBS was added to the slides, and after an incubation of 30 min in a humidified chamber, a wash with PBS was done. To counterstain the nuclei, slides were incubated for 10 min in 0.01% Hoechst 33342 (Sigma). After washes in PBS, air-drying, and mounting in Mowiol medium (Calbiochem), the slides were subjected to microscopic examination.

XV. Evaluation of Antitumor Efficacy. Balb Nu/Nu female mice from Harlan, Italy, 4−6 weeks old weighing 17−26 g, were maintained in cages with paper filter covers, food, sterilized bedding, and acidified water. A2780 human ovarian carcinoma (from American Type Culture Collection) was maintained by subcutaneous (sc) transplantation in athymic mice using 20−30 mg of tumor brei. For the experiment, tumors were excised and fragments were implanted sc into the left flank. The treatments started when the tumors were measurable; mean tumor weight for all the groups was 0.12 g. **41** was dissolved in 50% PEG400 (poly(ethylene glycol)) in glucose solution. Treatments were administered orally daily or twice a day for 10 days. In the control group, animals were treated with the vehicle twice a day. Every 3 days the tumor growth was evaluated. Tumor growth was assessed by caliper. The two diameters were recorded, and the tumor weight was calculated according to the following formula:

$$\text{tumor weight (mg)} = \frac{(\text{length, mm})(\text{width, mm})^2}{2}$$

The tumor growth inhibition (TGI, %) was calculated according to the equation

$$\%\ \text{TGI} = 100 - \frac{\text{mean tumor weight of treated group}}{\text{mean tumor weight of control group}} \times 100$$

Toxicity was evaluated on the basis of the body weight reduction. Mice were sacrificed when the tumors reached a volume that hampered them, and the gross autopsy findings, mainly the reduction of spleen and liver size, were reported.

Acknowledgment. We thank Dr. Daniela Borghi and Dr. Roberto Biancardi of the Analytical and Predevelopment Department of Pharmacia Italia for skillful assistance in NMR spectra recording and interpretation.

Supporting Information Available: Elemental analysis results of the compounds. This material is available free of charge via the Internet at http://pubs.acs.org.

References

(1) Hatakeyama, M.; Weinberg, R. A. The role of RB in cell cycle control. *Prog. Cell Cycle Res.* **1995**, *1*, 9−19.
(2) Morgan, D. O.; Fisher, R. P.; Espinoza, F. H.; Farrell, A.; Nourse, J.; Chamberlin, H.; Jin, P. Control of eukaryotic cell cycle progression by phosphorylation of cyclin-dependent kinases. *Cancer J. Sci. Am.* **1998**, *4* (Suppl. 1), S77−S83.
(3) Sherr, C. J. Cancer cell cycles. *Science* **1996**, *274*, 1672−1677.
(4) Malumbres, M.; Barbacid, M. To cycle or not to cycle: a critical decision in cancer. *Nat. Rev. Cancer* **2001**, *1* (3), 222−231.
(5) Tsutsui, T.; Hesabi, B.; Moons, D. S.; Pandolfi, P. P.; Hansel, K. S.; Koff, A.; Kiyokawa, H. Targeted disruption of CDK4 delays cell cycle entry with enhanced p27(Kip1) activity. *Mol. Cell. Biol.* **1999**, *19* (10), 7011−70199.
(6) Dynlacht, B. D.; Flores, O.; Lees, J. A.; Harlow, E. Differential regulation of E2F transactivation by cyclin/cdk2 complexes *Genes Dev.* **1994**, *8* (15), 1772−1786.
(7) Xu, M.; Sheppard, K. A.; Peng, C. Y.; Yee, A. S.; Piwnica-Worms, H. Cyclin A/CDK2 binds directly to E2F-1 and inhibits the DNA-binding activity of E2F-1/DP-1 by phosphorylation *Mol. Cell. Biol.* **1995**, *14* (12), 8420−8431.
(8) Pagano, M.; Pepperkok, R.; Verde, F.; Ansorge, W.; Draetta, G. Cyclin A is required at two points in the human cell cycle *EMBO J.* **1992**, *11* (3), 961−971.
(9) Donnellan, R.; Chetty, R. Cyclin E in human cancers. *FASEB J.* **1999**, *13* (8), 773−780.
(10) Tokuyama, Y.; Horn, H. F.; Kawamura, K.; Tarapore, P.; Fukasawa, K. Specific phosphorylation of nucleophosmin on Thr-(199) by cyclin-dependent kinase 2-cyclin E and its role in centrosome duplication. *J. Biol. Chem.* **2001**, *276* (24), 21529−21537. Meraldi, P.; Lukas, J.; Fry, A. M.; Bartek, J.; Nigg, E. A. Centrosome duplication in mammalian somatic cells requires E2F and Cdk2-cyclin A *Nat. Cell Biol.* **1999**, *1* (2), 88−93.
(11) Hall, C.; Nelson, D. M.; Ye, X.; Baker, K.; DeCaprio, J. A.; Seeholzer, S.; Lipinski, M.; Adams, P. D. HIRA, the human homologue of yeast Hir1p and Hir2p, is a novel cyclin-cdk2 substrate whose expression blocks S-phase progression *Mol. Cell. Biol.* **2001**, *21* (5), 1854−1865.
(12) Zhao, J.; Kennedy, B. K.; Lawrence, B. D.; Barbie, D. A.; Matera, A. G.; Fletcher, J. A.; Harlow, E. NPAT links cyclin E-Cdk2 to the regulation of replication-dependent histone gene transcription. *Genes Dev.* **2000**, *14* (18), 2283−2297.
(13) Okuda, M.; Horn, H. F.; Tarapore, P.; Tokuyama, Y.; Smulian, A. G.; Chan, P. K.; Knudsen, E. S.; Hofmann, I. A.; Snyder, J. D.; Bove, K. E.; Fukasawa, K. Nucleophosmin/B23 is a target of CDK2/cyclin E in centrosome duplication *Cell* **2000**, *103* (1), 127−140.
(14) Pagano, M.; Pepperkok, R.; Lukas, J.; Baldin, V.; Ansorge, W.; Bartek, J.; Draetta, G. Regulation of the cell cycle by the cdk2 protein kinase in cultured human fibroblasts. *J. Cell Biol.* **1993**, *121* (1), 101−111. Girard, F.; Strausfeld, U.; Fernandez, A.; Lamb, N. J. Cyclin A is required for the onset of DNA replication in mammalian fibroblasts. *Cell* **1991**, *67* (6), 1169−1179.
(15) Kitagawa, M.; Higashi, H.; Suzuki-Takahashi, I.; Segawa, K.; Hanks, S. K.; Taya, Y.; Nishimura, S.; Okuyama, A. Phosphorylation of E2F-1 by cyclin A-cdk2. *Oncogene* **1995**, *10* (2), 229−236.
(16) Krek, W.; Xu, G.; Livingston, D. M. Cyclin A-kinase regulation of E2F-1 DNA binding function underlies suppression of an S phase checkpoint. *Cell* **1995**, *83* (7), 1149−1158. Xu, M.; Sheppard, K. A.; Peng, C. Y.; Yee, A. S.; Piwnica-Worms, H. Cyclin A/CDK2 binds directly to E2F-1 and inhibits the DNA-binding activity of E2F-1/DP-1 by phosphorylation. *Mol. Cell. Biol.* **1994**, *14* (12), 8420−8431.
(17) DeGregori, J.; Leone, G.; Miron, A.; Jakoi, L.; Nevins, J. R. Distinct roles for E2F proteins in cell growth control and apoptosis *Proc. Natl. Acad. Sci. U.S.A.* **1997**, *94* (14), 7245−7250.
(18) Chen, Y. N.; Sharma, S. K.; Ramsey, T. M.; Jiang, L.; Martin, M. S.; Baker, K.; Adams, P. D.; Bair, K. W.; Kaelin, W. G., Jr. Selective killing of transformed cells by cyclin/cyclin-dependent kinase 2 antagonists *Proc. Natl. Acad. Sci. U.S.A.* **1999**, *96* (8), 4325−4329.
(19) Tsihlias, J.; Kapusta, L.; Slingerland, J. The prognostic significance of altered cyclin-dependent kinase inhibitors in human cancer. *Annu. Rev. Med.* **1999**, *50*, 401−423.
(20) Lloyd, R. V.; Erickson, L. A.; Jin, L.; Kulig, E.; Qian, X.; Cheville, J. C.; Scheithauer, B. W. p27kip1: a multifunctional cyclin-dependent kinase inhibitor with prognostic significance in human cancers. *Am. J. Pathol.* **1999**, *154* (2), 313−323.
(21) Tetsu, O.; McCormick, F. Proliferation of cancer cells despite CDK2 inhibition. *Cancer Cell* **2003**, *3* (3), 233−245.
(22) Senderowicz, A. M. Small-molecule cyclin-dependent kinase modulators *Oncogene* **2003**, *22* (42), 6609−6620.
(23) Zhai, S.; Senderowicz, A. M.; Sausville, E. A.; Figg, W. D. Flavopiridol, a novel cyclin-dependent kinase inhibitor, in clinical development. *Ann. Pharmacother.* **2002**, *36*, 905−911.
(24) McClue, S. J.; Blake, D.; Clarke, R.; Cowan, A.; Cummings, L.; Fischer, P. M.; MacKenzie, M.; Melville, J.; Stewart, K.; Wang, S.; Zhelev, N.; Zheleva, D.; Lane, D. P. In vitro and in vivo antitumor properties of the cyclin dependent kinase inhibitor CYC202 (*R*-roscovitine). *Int. J. Cancer* **2002**, *102* (5), 463−468.
(25) Misra, R. N.; Xiao, H.-Y.; Kim, K. S.; Lu, S.; Han, W.-C.; Rawlins, D. B.; Shan, W.; Ahmed, S. Z.; Qian, L.; Chen, B.-C.; Zhao, R.; Bednarz, M. S.; Bursuker, I.; Kellar, K. A.; Mulheron, J. G.; Batorsky, R. K.; Kamath, A.; Humphreys, W. G.; Marathe, P.; Hunt, J. T.; Pavletich, N. P.; Kimball, S. D.; Webster, K. R. BMS-387032: A selective cdk2 inhibitor with potent antitumor activity. *Abstracts of Papers*, 225th National Meeting of the American Chemical Society, New Orleans, LA, March 23−27, 2003.

(26) Pevarello, P.; Orsini, P.; Traquandi, G.; Varasi, M.; Fritzen, E. L.; Warpehoski, M. A.; Pierce, B. S.; Brasca, M. G.3(5)-Acylaminopyrazole derivatives, process for their preparation and their use as antitumor agents. International Patent WO 01/12189.
(27) Seelen, W.; Schäfer, M.; Ernst, A. Selective ring N-protection of aminopyrazoles. *Tetrahedron Lett.* **2003**, *44*, 4491−4493.
(28) De Azevedo, W. F.; Leclerc, S.; Meijer, L.; Havlicek, L.; Strnad, M.; Kim, S. H. Inhibition of cyclin-dependent kinases by purine analogues: crystal structure of human cdk2 complexed with roscovitine. *Eur. J. Biochem*. **1997**, *243* (1−2), 518−26.
(29) Pavletich, N. P. Mechanisms of cyclin-dependent kinase regulation: structures of Cdks, their cyclin activators, and Cip and INK4 inhibitors. *J. Mol. Biol*. **1999**, *287* (5), 821−828.
(30) Ling, V. Multidrug resistance: molecular mechanisms and clinical relevance. *Cancer Chemother. Pharmacol.* **1997**, *40* (Suppl.), S3−S8.
(31) For a general discussion, see the following. Baguley, B. C.; Hicks, K. O.; Wilson, W. R. Tumor cell cultures in drug development. In *Anticancer Drug Development*; Baguley, B. C., Kerr, D. J., Eds.; Academic Press: San Diego, CA, 2002; pp 269−284.
(32) Isacchi, A. Manuscript in preparation.
(33) Skehan, P.; Storeng, R.; Scudiero, D.; Monks, A.; McMahon, J.; Vistica, D.; Warren, J. T.; Bokesch, H.; Kenney, S.; Boyd, M. R. New colorimetric cytotoxicity assay for anticancer-drug screening. *J. Natl. Cancer Inst.* **1990**, *82*, 1107−1112.
(34) Jeffrey, P. D.; Russo, A. A.; Polyak, K.; Gibbs, E.; Hurwitz, J.; Massague, J.; Pavletich, N. P. Mechanism of CDK activation revealed by the structure of a cyclinA-CDK2 complex. *Nature* **1995**, *376*, 313−320.
(35) Otwinowski, Z.; Minor, W. Processing of X-ray Diffraction Data Collected in Oscillation Mode. *Methods in Enzymology*; Academic Press: New York, 1997; Vol. 276.
(36) Brünger, A. T.; Adams, P. D.; Clore, G. M.; DeLano, W. L.; Gros, P.; Grosse-Kunstleve, R. W. Crystallography and NMR system: a new software suite for macromolecular structure determination. *Acta Crystallogr., Sect. D* **1998**, *54*, 905−921.
(37) Rosenblatt, J.; De Bondt, H.; Jancarik, J.; Morgan, D. O.; Kim, S. H. Purification and crystallization of human cyclin-dependent kinase 2. *J. Mol. Biol*. **1993**, *230* (4), 1317−1319.
(38) Lawrie, A. M.; Noble, M. E. M.; Tunnah, P.; Brown, N. R.; Johnson, L. N.; Endicott, J. A. Protein kinase inhibition by staurosporine revealed in details of the molecular interaction with CDK2. *Nat. Struct. Biol.* **1997**, *4*, 796−801.
(39) Kleywegt, G. J.; Jones, T. A. Phi/psi-chology: Ramachandran revisited. *Structure* **1996**, *4*, 1395−1400.

JM031145U